frontiers in Earth Science

ORIGINAL RESEARCH
published: 08 January 2021
doi: 10.3389/feart.2020.600976

# Age and Paleoenvironmental Significance of the Frazer Beach Member—A New Lithostratigraphic Unit Overlying the End-Permian Extinction Horizon in the Sydney Basin, Australia

*Stephen McLoughlin[1]*, Robert S. Nicoll[2], James L. Crowley[3], Vivi Vajda[1], Chris Mays[1], Christopher R. Fielding[4], Tracy D. Frank[4], Alexander Wheeler[5] and Malcolm Bocking[6]*

[1]Department of Paleobiology, Swedish Museum of Natural History, Stockholm, Sweden, [2]Independent Researcher, Bungendore, NSW, Australia, [3]Isotope Geology Laboratory, Boise State University, Boise, ID, United States, [4]Department of Earth and Atmospheric Sciences, University of Nebraska-Lincoln, Lincoln, NE, United States, [5]School of Earth and Environmental Sciences, The University of Queensland, St. Lucia, QLD, Australia, [6]Bocking Associates, Castle Hill, NSW, Australia

OPEN ACCESS

**Edited by:**
*Evelyn Kustatscher, Museum of Nature South Tyrol, Italy*

**Reviewed by:**
*Johann Neveling, Council for Geoscience, South Africa*
*Cindy Virginia Looy, University of California, Berkeley, United States*

***Correspondence:**
*Stephen McLoughlin*
*steve.mcloughlin@nrm.se*

**Specialty section:**
*This article was submitted to Paleontology, a section of the journal Frontiers in Earth Science*

**Received:** *31 August 2020*
**Accepted:** *11 November 2020*
**Published:** *08 January 2021*

**Citation:**
*McLoughlin S, Nicoll RS, Crowley JL, Vajda V, Mays C, Fielding CR, Frank TD, Wheeler A and Bocking M (2021) Age and Paleoenvironmental Significance of the Frazer Beach Member—A New Lithostratigraphic Unit Overlying the End-Permian Extinction Horizon in the Sydney Basin, Australia. Front. Earth Sci. 8:600976. doi: 10.3389/feart.2020.600976*

The newly defined Frazer Beach Member of the Moon Island Beach Formation is identified widely across the Sydney Basin in both outcrop and exploration wells. This thin unit was deposited immediately after extinction of the *Glossopteris* flora (defining the terrestrial end-Permian extinction event). The unit rests conformably on the uppermost Permian coal seam in most places. A distinctive granule-microbreccia bed is locally represented at the base of the member. The unit otherwise consists of dark gray to black siltstone, shale, mudstone and, locally, thin lenses of fine-grained sandstone and tuff. The member represents the topmost unit of the Newcastle Coal Measures and is overlain gradationally by the Dooralong Shale or with a scoured (disconformable) contact by coarse-grained sandstones to conglomerates of the Coal Cliff Sandstone, Munmorah Conglomerate and laterally equivalent units. The member is characterized by a palynological "dead zone" represented by a high proportion of degraded wood fragments, charcoal, amorphous organic matter and fungal spores. Abundant freshwater algal remains and the initial stages of a terrestrial vascular plant recovery flora are represented by low-diversity spore-pollen suites in the upper part of the unit in some areas. These assemblages are referable to the *Playfordiaspora crenulata* Palynozone interpreted as latest Permian in age on the basis of high precision Chemical Abrasion Isotope Dilution Thermal Ionization Mass Spectrometry (CA-IDTIMS) dating of thin volcanic ash beds within and stratigraphically bracketing the unit. Plant macrofossils recovered from the upper Frazer Beach Member and immediately succeeding strata are dominated by *Lepidopteris* (Peltaspermaceae) and *Voltziopsis* (Voltziales) with subsidiary pleuromeian lycopsids, sphenophytes, and ferns. Sparse vertebrate and invertebrate ichnofossils are also represented in the Frazer Beach Member or in beds immediately overlying this unit. The Frazer Beach Member is correlative, in part, with a thin interval of organic-rich mudrocks, commonly known as

the "marker mudstone" capping the Permian succession further to the north in the Bowen, Galilee and Cooper basins. The broad geographic distribution of this generally <5-m-thick mudrock unit highlights the development in eastern Gondwana of extensive, short-lived, shallow lacustrine systems with impoverished biotas in alluvial plain settings in the immediate aftermath of the end-Permian biotic crisis.

**Keywords: Permian-Triassic, mass extinction, CA-IDTIMS, plant fossils, palynology, fluvial sedimentology, stable isotope geochemistry, anachronistic facies**

## INTRODUCTION

Coalfield geologists in New South Wales, Australia, have long recognized a unit of dark gray to black shales, mudstones and siltstones, typically <2m thick, capping the uppermost Permian coal seam across the Sydney Basin. Historically, this interval has been termed the Bulli or Vales Point "roof strata" (Diessel et al., 1967), "roof shales" (Townrow, 1967b; White, 1981), "transitional zone/beds" (Hennelly, 1958; Wu et al., 2019), "blacks" (in part: Clark, 1992) or, in a paleontological sense, the "dead zone" (Vajda et al., 2020). Traditionally, the top of the uppermost Permian coal seam has been used to define the boundary between the Newcastle Coal Measures (and Illawarra Coal Measures in southern and western regions of the basin) and the overlying Narrabeen Group (Agnew et al., 1995; Armstrong et al., 1995; Scheibner and Basden, 1998; Creech, 2002; Shi et al., 2010; Pinetown, 2014; Metcalfe et al., 2015; Laurie et al., 2016). Consequently, previous studies have assigned the Vales Point/Bulli "roof strata" to the basal Narrabeen Group. In contrast, Hutton and Bamberry (1999, p. 122) recommended that these carbonaceous mudrocks should be treated as part of the Sydney Subgroup (uppermost Newcastle/Illawarra Coal Measures), but the unit has never been formally defined.

The boundary between the Bulli/Katoomba/Vales Point coal seams and the overlying shale/siltstone interval marks a major change in fossil floras throughout the Sydney Basin and is the terrestrial expression of the end-Permian extinction event (EPE) (Grebe, 1970; Helby, 1973; Retallack, 1977; Fielding et al., 2019; Mays et al., 2020; Vajda et al., 2020). Recently, our team and others have noted that this shale/mudstone/siltstone unit represents a distinctive lacustrine facies association (Facies Association G of Fielding et al., 2020) overprinted by paleosol development (Retallack, 2005), and is characterized by excursions in the values of carbon stable isotopes and chemical index of alteration (CIA) (Williams et al., 2017; Vajda et al., 2020). The unit hosts distinctive vertebrate ichnofossil (Retallack 1996; McLoughlin et al., 2020), and palynofloral assemblages initiating with a post-extinction "dead zone" primarily incorporating coalified wood and charcoal fragments. Higher in this interval, and in overlying units, abundant fungal, algal and sparse fern palynomorphs characterize post-extinction communities of opportunistic plants and the initial stages of a recovery flora (Fielding et al., 2020; Mays et al., 2020; Vajda et al., 2020).

Historically, the EPE and Permian-Triassic boundary (PTB) were assumed to be coincident across the Sydney Basin for mapping purposes and placed at the top of the uppermost Permian coal seam (McElroy, 1969). However, early palynological studies employing floristic correlations with other regions (Evans, 1966; Balme, 1969; Helby, 1970; Helby, 1973; Helby et al., 1987) inferred the PTB to be positioned higher (within the Narrabeen Group) than the major floral turnover (EPE). Some workers have invoked a significant hiatus and an erosional unconformity around the Permian-Triassic transition (base of the Narrabeen Group) in various parts of the basin (Rattigan and McKenzie, 1969; Helby, 1970; Helby, 1973; Herbert, 1997), whereas others argued that the transition is conformable (Dun, 1910). Recent work integrating sedimentology, palynostratigraphy and high-precision CA-IDTIMS dating of zircon crystals from ash beds shows that the transition is generally conformable in the basin's main depocenters and provides clarity to the positions of the EPE and PTB within the succession (Metcalfe et al., 2015; Fielding et al., 2019; Fielding et al., 2020; Mays et al., 2020; Vajda et al., 2020).

Given that this package of mudrocks is lithologically distinct from the bracketing coal and sandstone units, has a unique fossil content, has a broad geographic distribution, and is positioned in an interval of global interest (between the EPE and PTB horizons), we argue that it deserves recognition as a discrete lithostratigraphic unit. Here we formally describe this unit as the Frazer Beach Member of the Moon Island Beach Formation and raise the Newcastle/Illawarra Coal Measures boundary to the top of this new unit. We document the sedimentary characteristics, fossil biota, depositional setting, regional correlative units and global paleoenvironmental significance of this member.

## MATERIAL AND METHODS

Sedimentological features and stratigraphic relationships were compiled by logging numerous outcrop sections and bore cores from sites across the Sydney Basin (see Fielding et al., 2020 for details). Additional data were obtained from various downhole geophysical logs and well completion reports for boreholes distributed widely through the Sydney Basin and contiguous basins to the north (Gunnedah, Bowen, Galilee, and Cooper basins).

Plant macrofossils were studied from beds overlying the Bulli and Vales Point coal seams exposed at various sites around the Sydney Basin (**Figure 1D**) and now held in the Australian Museum (Sydney: prefixed AMF) and Swedish Museum of Natural History (Stockholm: prefixed S). Specimens were examined and photographed with low-angle light using a

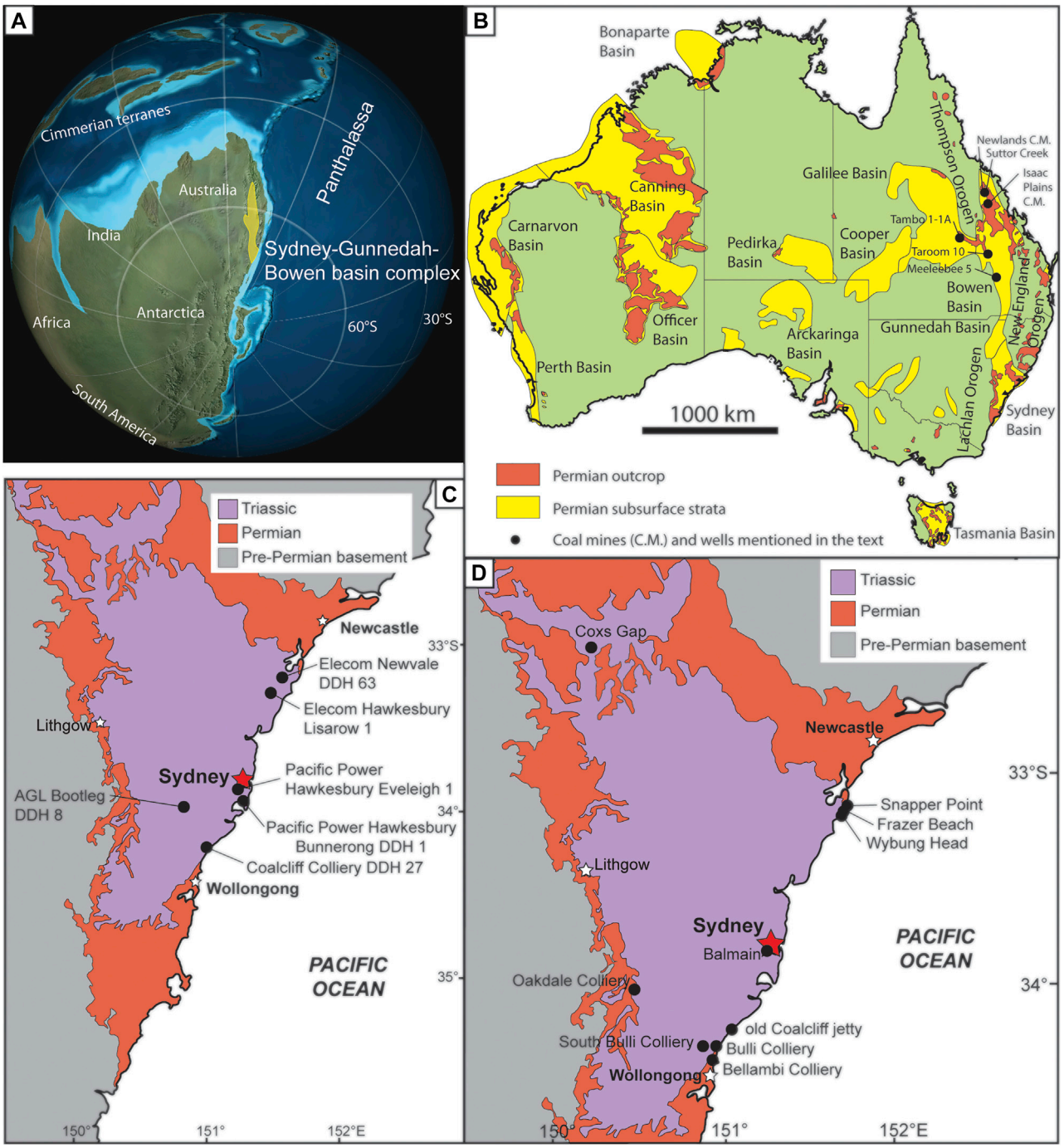


**FIGURE 1 |** Locality maps. **(A)**, Paleogeographic map showing the position of the Sydney-Gunnedah-Bowen Basin complex in southeastern Gondwana. **(B)**, Map of eastern Australia showing the distribution of Permian–Triassic basins. **(C)**, Map of the Sydney Basin showing key wells mentioned in the text. **(D)**, Map of the Sydney Basin showing key outcrop localities mentioned in the text.

Canon Eos 40D camera. Palynoassemblages were studied from several wells and outcrop sections (**Figure 1C**): Pacific Power Hawkesbury Bunnerong DDH 1 (PHKB-1), central Sydney Basin (lat: 33°58′17.61″S, long: 151°13′43.52″E); AGL Bootleg DDH 8 (AGLB-8), central Sydney Basin (lat: 34°00′36″S, long: 150°44′28″E); Coalcliff Colliery DDH 27 (CCC-27), southern Sydney Basin (lat: 34°13′25.28″S, long: 150°56′50.67″E), Elecom Hawkesbury Lisarow 1 (EHKL-1), northern Sydney Basin (lat: 33°22′38.54″S, long: 151°23′0.53″E); exposures at Coal Cliff (lat: 34°15′18.9″S, long: 150°58′22.2″E), southern Sydney Basin, and Snapper Point (lat: 33°11′13.35″S, long: 151°37′42.00″E) and Frazer Beach (lat: 33°11′37.21″S, long: 151°37′22.34″E),

Munmorah State Conservation Area, northern Sydney Basin. Core samples were obtained for palynology from the W.B. Clarke Geoscience Center drillcore library, Londonderry, New South Wales, Australia. Samples of ~10–25 g were processed for palynology according to standard procedures at Global Geolab Limited, Canada (see Mays et al., 2020; Vajda et al., 2020 for details). Palynomorphs were imaged using a Zeiss Axioskop 2 Plus transmitted light microscope equipped with a Zeiss AxioCam MRc camera or an Olympus BX51 transmitted light microscope with a Lumenera Infinity 2 digital camera. All palynological slides are housed at the Department of Palaeobiology, Swedish Museum of Natural History.

The total organic carbon (TOC) concentration and carbon-isotopic composition of bulk organic matter was determined on splits of samples used for palynological analyses. Samples were initially powdered using a Sibtechnik rock pulverizer, then reacted with 1 N HCl for 24 h to remove inorganic carbon, rinsed three times in Milli Q water, dried at 40°C, and repowdered with an agate mortar and pestle. Powders were analyzed using a Costech Elemental Analyzer connected to a Thermo Finnigan MAT 253 Isotope Ratio Mass Spectrometer at the Keck-NSF Paleoenvironmental and Environmental Laboratory, University of Kansas. Carbon-isotopic compositions of bulk organic matter fractions are reported in permil (‰) relative to VPDB. Analyses of working standards (DORM, ATP) were reproducible to better than ±0.13‰ ($1\sigma$ SD) for $\delta^{13}C_{org}$.

The Chemical Index of Alteration (CIA) of Nesbitt and Young (1982) tracks the conversion of feldspars to clays via hydration during the weathering of fine-grained siliciclastics (Sheldon and Tabor, 2009). Whereas fresh crystalline rocks are characterized by relatively low CIA values (45–55), leaching of mobile oxides and concentration of $Al_2O_3$ during chemical weathering causes CIA values to approach 100. The CIA is calculated using the following equation:

$$\mathrm{CIA} = 100 \times \frac{\mathrm{Al_2O_3}}{\mathrm{Al_2O_3 + CaO^* + K_2O + Na_2O}},$$

wherein oxides are in molar units and CaO* represents the CaO in the silicate fraction following the method of McLennan (1993). Elemental concentrations used to calculate the CIA were measured using a Bruker Tracer 5i portable x-ray fluorescence (XRF) analyzer calibrated with a series of mudrock standards including USGS shale standards SBC-1 and SCO-2, a suite of mudrock reference materials characterized by Rowe et al. (2012), and nine in-house reference materials from Permo-Triassic mudrocks in the Pacific Hawkesbury Bunnerong DDH-1 (PHKB1) drill core from the Sydney Basin, NSW described by Fielding et al. (2019). Samples were analyzed four times using a Bruker Tracer 5i in the Sedimentary Geochemistry Laboratory at the University of Nebraska-Lincoln, twice under low-energy and twice under high-energy conditions with different filters, to target a series of overlapping Kα ranges and enable precise analysis of relatively light and heavy elements. The elements Na to Fe on the periodic table were analyzed with no filter at 15 kV and 15 μA and a count time of 30 s. Concentrations of Na and Mg were also measured under a helium flush to negate atmospheric interference. High-energy analyses were undertaken at 50 kV and 35 μA and a count time of 30 s, with a Cu 75 μm:Ti 25 μm:Al 200 μm filter for the elements Ca to Kr and a Cu 100 μm:Ti 25 μm:Al 200 μm filter for Co and higher on the periodic table. The raw count rate per second (rcps) signals lay between 20,000 and 100,000 rcps.

CA-IDTIMS dating of zircons from various tuff and tuffaceous shale beds pertinent to this study was carried out at the Isotope Geology Laboratory, Boise State University, ID, USA. Details of processing methods, U-Pb isotopic data, individual grain ages, and measures of uncertainty were provided by Metcalfe et al. (2015), Fielding et al. (2019), and Fielding et al. (2020).

## TECTONIC SETTING

The Sydney-Gunnedah-Bowen basin complex represents a large Permo-Triassic meridional foreland basin system positioned between the New England Orogen (a continental volcanic arc to the east) and the cratonized lower–middle Paleozoic Lachlan and Thomson orogens (to the west). The basin system developed under a convergent tectonic regime related to subduction of Panthalassan oceanic crust along the southeast margin of Gondwana (**Figure 1A**). The sedimentary fill of this basin complex shares various depositional features with adjacent epicratonic basins to the west (e.g., the Galilee, Cooper, Pedirka, and Arckaringa basins), and the Tasmania Basin to the south (**Figure 1B**).

The Sydney Basin spans >60,000 $km^2$ at the southern end of the foreland basin system. It was located at high paleolatitudes during the Permian–Triassic transition: at ~65–75°S according to (Veevers, 2006) or ~85–90°S (according to Klootwijk, 2016). The basin hosts >5,000 m of basal Permian to Middle Triassic strata incorporating Cisuralian and Guadalupian glacigene and marine sedimentary rocks from the waning phase of the Late Paleozoic Ice Age, extensive coal-bearing coastal and alluvial plain deposits of the Lopingian, and fully alluvial systems in the Triassic (Tadros, 1995). Sedimentation terminated with the culmination of the Hunter-Bowen Orogeny toward the end of the Ladinian. Extensive tuffs from volcanic eruptions along the New England Fold Belt are incorporated within the Sydney Basin succession and facilitate absolute dating of the strata and calibration of the local palynostratigraphic zonation, which represents the standard reference scheme for eastern Gondwana.

## LITHOSTRATIGRAPHY

### Singleton Supergroup

The Singleton Supergroup was formalized by Moffitt (1982). In the Newcastle Coalfield (northeastern Sydney Basin), it is normally employed for the marine and coal-bearing succession (Tomago and Newcastle coal measures) between the underlying Maitland Group and overlying Narrabeen Group (Stephenson and Burch, 2004).

### Newcastle Coal Measures (Group Status)

Although upper Permian coal has been mined in the Sydney Basin since the late 1700s, the first comprehensive study of the

Newcastle Coal Measures was by David (1907) based on two decades of investigations. Geological studies progressed through the early 20th century with growing exploration for, and exploitation of, Permian bituminous coal, but an integrated lithostratigraphic scheme spanning the entire basin proved difficult to attain. Instead, separate schemes were established in each of the major coal-mining districts. Fairbridge (1953) provided one of the first attempts to categorize the Newcastle Coal Measures in detail and the unit was formally defined by Booker (1960). Key subdivisions of the coal measures were proposed by McKenzie and Britten (1969), modified by the Standing Committee on Coalfield Geology of NSW (1975), and thoroughly revised by Ives et al. (1999) based on a meridional transect of boreholes roughly 5–20 km from the coast through the northern Sydney Basin.

Ives et al. (1999) re-defined the base of the Newcastle Coal Measures as the top of the Waratah Sandstone, constituting a more sharply delimited lithological change than the gradational base of this sandy unit used previously as the floor of the coal measures. Until the 1990s, the top of the Newcastle Coal Measures had been placed at the cap of the Wallarah coal seam (placing the "Cowper tuff," "Karignan conglomerate" and Vales Point coal seam in the Narrabeen Group). Ives et al. (1999) re-defined the top of the Newcastle Coal Measures to correspond to the top of the uppermost coal seam—in most areas, this is the Vales Point coal seam but, locally, the upper limit is retained at the top of the Wallarah coal seam where the two uppermost seams merge or the Vales Point coal seam, "Karignan conglomerate" and "Cowper tuff" have been removed by erosion or pinch out laterally. They recognized this upper boundary to mark a distinctive lithological transition in that mottled gray-green-red mudrocks, typical of the overlying Narrabeen Group, do not occur below the Vales Point coal seam. They also argued that there is a vertical change in conglomerate texture from loosely packed small- to medium-sized pebbles, to tightly packed small to large pebbles and cobbles above this level, especially in the northern part of the basin. This revised placement of the upper boundary was suggested earlier by Uren (1974). Ives et al. (1999) re-designated all previously established coal formations as informal coal seams and removed formation status for all other small internal units except for the Warners Bay Tuff. They redefined previously established subgroups and recognized them as formations, viz., the Lambton, Adamstown, Boolaroo and Moon Island Beach formations in ascending stratigraphic order (**Figures 2A,B**). These formations were respectively separated by prominent tuffaceous units, viz., Nobbys Tuff, Warners Bay Tuff, and Awaba Tuff, the first and last of which were raised to formation status. These thick tuffaceous units are distributed extensively in the northern Sydney Basin and represent key time markers across the region. The lithostratigraphic scheme of Ives et al. (1999) is simpler and more consistent than previous frameworks but we note that it reduces some members widely recognized in older studies (e.g., the Karignan Conglomerate and Cowper Tuff members) to informal status. We argue that stratigraphic communication would be facilitated by recognizing such well-categorized units as formal members of the formations established by Ives et al. (1999).

## Moon Island Beach Formation

This term was first used by Slansky (1985) and defined by Ives et al. (1999) as a partial replacement of the Moon Island Beach Subgroup of McKenzie and Britten (1969). The type section is defined as the interval from 116.41 to 187.345 m in the Elecom Newvale DDH 63 Well. The formation consists of interbedded sandstone, shale, conglomerate, claystone, and coal, and extends south and west from coastal outcrops near Catherine Hill Bay, Swansea, Belmont North, Awaba, Fassifern, Teralba and along the Sugarloaf Range south from Mount Sugarloaf in the northern Sydney Basin. The base is defined as the top of the Awaba Tuff and the top was originally defined as the top of the Vales Point coal seam or its lateral equivalents. Here we extend the upper boundary of this formation to the top of the newly defined Frazer Beach Member.

## Vales Point Coal Seam and Bulli Coal

We discuss these units owing to their intimate depositional relationship with the overlying Frazer Beach Member. The Vales Point coal seam represents an informally defined unit positioned previously at the top of the Newcastle Coal Measures (**Figure 2B**). It was first referred to in this syntax by Scheibner and Basden (1998), but has also been called the "Vales Point Coal Member" (Bryan et al., 1966), "Vales Point Coal Seam" (McKenzie and Britten, 1969), "Vales Point Coal Seam Member" (Branagan, 1972), "Vales Point Coal" (Foster, 1979) and "Vales Point seam" (Creech, 2002). It merges with the underlying Wallarah coal seam in places where the intervening "Karignan conglomerate" is absent. We retain the Vales Point coal seam under informal nomenclature following Ives et al. (1999) but note that its recognition as a formal member would provide a clearer stratigraphic hierarchy. It consists of banded bituminous coal generally 0.5–1 m thick but locally reaching 5 m thick where it merges with the underlying Wallarah coal seam. The Vales Point coal seam has a dulling-up profile and at some sites contains thin laminae of dark shale. The uppermost few cm are blocky and commonly stained at the top and along joints by iron oxides or sulfates.

In the southern Sydney Basin, the Bulli Coal is stratigraphically equivalent to the Vales Point coal seam (**Figure 2B**). It is typically represented by 2–3 m of well-banded bituminous coal with sporadic carbonaceous mudstone and sideritic interbeds (Clark, 1992; Armstrong et al., 1995). The uppermost ply of the Bulli Coal is a coaly or highly carbonaceous shale commonly called the "blacks" in local miners' parlance and is indicative of changing depositional environments toward the termination of peat accumulation (Diessel et al., 1967; Clark, 1992). This ply is commonly gradational with the underlying part of the Bulli Coal and is overlain sharply or gradationally by shale (of the Frazer Beach Member) or erosionally by coarse-grained sedimentary rocks (of the Coal Cliff Sandstone). The "blacks" appears to be, in part or in whole, correlative with the basal granulestone/microbreccia bed of the Frazer Beach Member type section.

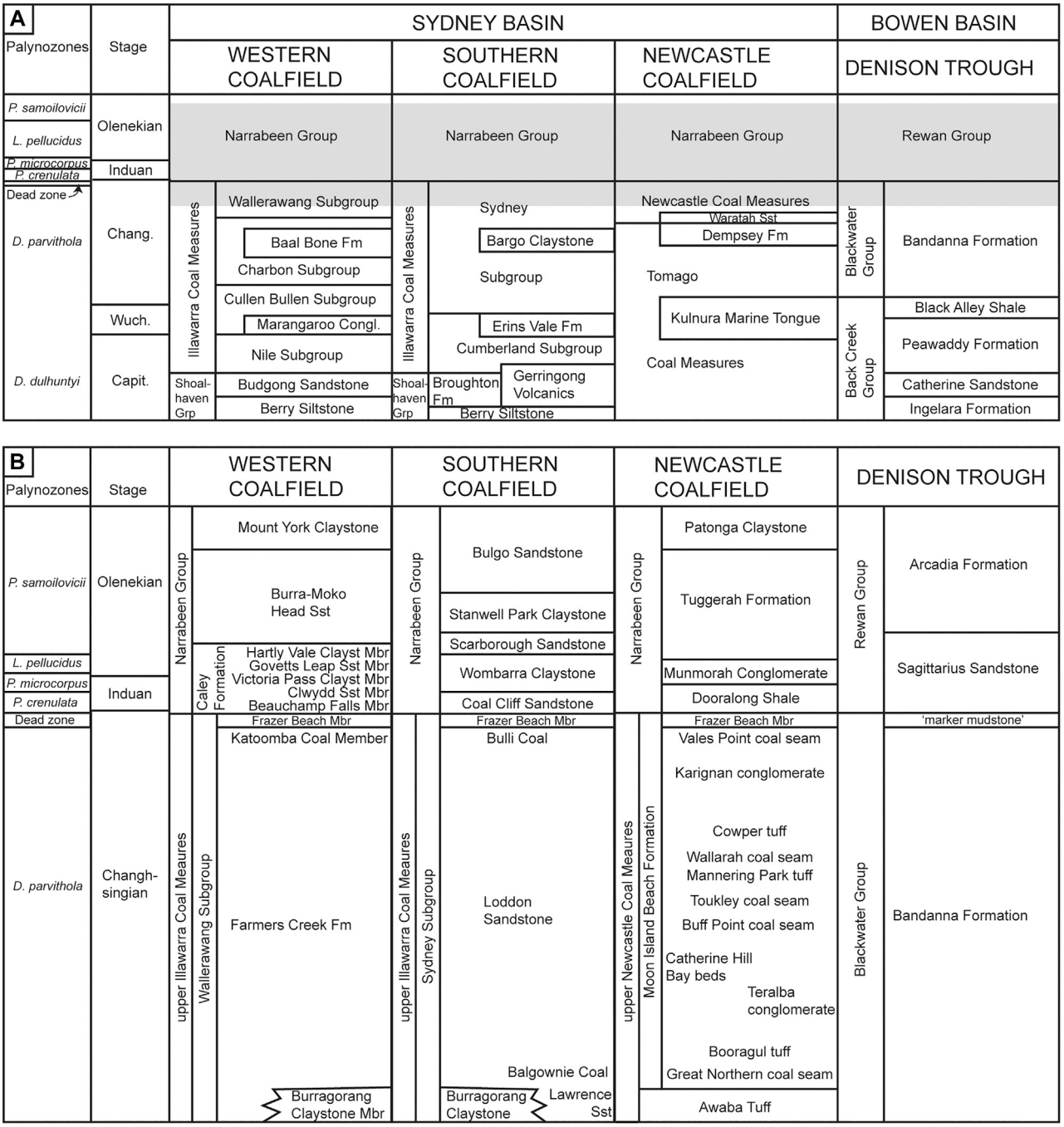


**FIGURE 2 |** Simplified stratigraphic correlation charts for Middle Permian to Lower Triassic strata of the southern, western, and northern (Newcastle Coalfield) parts of the Sydney Basin, and adjacent Bowen Basin. **(A)**, Correlation of major lithostratigraphic units. **(B)**, Correlation of minor formal and informal lithostratigraphic units for the interval marked in gray within panel **(A)**. Precise correlation of uppermost Permian units across the basin complex is currently unresolved. Adapted from Agnew et al. (1995), Armstrong et al. (1995), Yoo et al. (1995) and Ives et al. (1999).

## Frazer Beach Member (New Unit)

### Justification

In the course of fieldwork in the Sydney Basin, we recognized a distinct, thin, laterally persistent unit of dark mudrocks overlying the Vales Point coal seam but resting below the first major sandstone, conglomerate, or gray-green-red mottled mudrocks typical of the Narrabeen Group. In its organic-rich composition and conformable or gradational base it has stronger developmental affinities to the underlying strata than it does to overlying successions with which it has a locally erosional contact. On this basis, we recognize this distinctive package of strata as a new formal subunit—the Frazer Beach Member

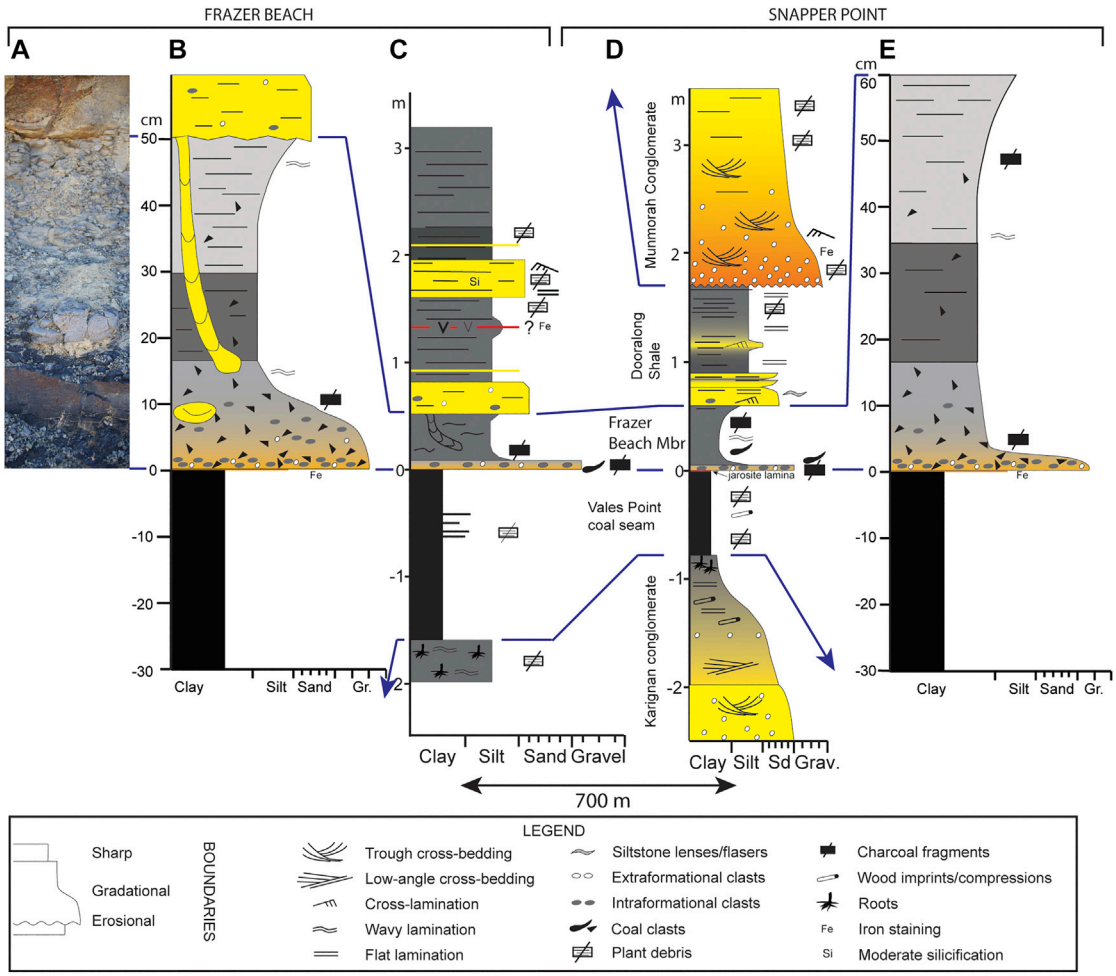


**FIGURE 3 |** Type section of the Frazer Beach Member at Frazer Beach. **(A)**, outcrop photo. **(B)**, Graphic log at the same scale. **(C)**, Graphic log showing relationships to stratigraphically adjacent units. **(D)**, Graphic log of secondary reference section at Snapper Point 700 m to the north of the type section showing relationships to stratigraphically bounding units. **(E)**, Enlargement of graphic log of the Frazer Beach Member at Snapper Point.

(FBM)—of the Moon Island Beach Formation. In doing so, we raise the top of the Moon Island Beach Formation, and by definition, the Newcastle Coal Measures and Singleton Supergroup, to be defined by the base of the first major channel sandstone or its lateral equivalent—variably a massive fine-grained sandstone splay deposit or interval of interlaminated fine-grained sandstones and gray siltstones constituting the base of the Dooralong Shale—of the Narrabeen Group.

This new member has stratigraphic value as a distinctive marker unit blanketing much of the Sydney Basin and is coeval with equivalent facies (informally termed the "marker mudstone") in sedimentary basins of northeastern Australia. Recognition of the FBM also aids documentation of the biotic and environmental changes expressed between the EPE and PTB in eastern Australia. Formalizing the unit also facilitates communication with geotechnicians, as beds of this member provide roof stability in mining operations exploiting the uppermost Permian coals in the Sydney Basin.

## Etymology

Named after the location of the type section at Frazer Beach, in the Munmorah State Conservation Area, New South Wales, Australia.

## Type Section

Coastal cliff section at 33°11′37.21″S, 151°37′22.34″E, logged by Fielding et al. (2019 figure 3), Vajda et al. (2020 figure 3), Fielding et al. (2020 figure 10) and illustrated in expanded form here (**Figures 3A–C**).

## Additional Reference Sections

Secondary reference sections are designated in coastal exposures at Snapper Point, 700 m to the north of the type section (**Figures 3D,E**), and at Coalcliff in the southern Sydney Basin (34°15′18.9″S, 150°58′22.2″E; **Figures 4A,B**). In the latter, the FBM rests sharply but conformably on the Bulli Coal and is overlain with an erosional contact by channel sandstones

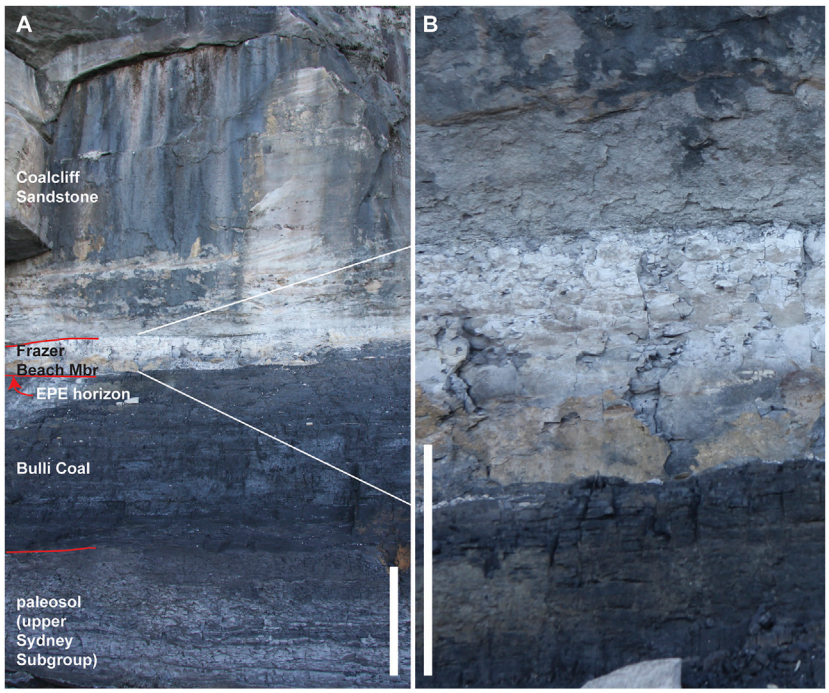


**FIGURE 4 |** Outcrop photos of the secondary reference section of the Frazer Beach Member above the Bulli Coal at Coal Cliff in the southern Sydney Basin. **(A)**, Frazer Beach Member represented as a persistent siltstone band above the Bulli Coal and below the multistorey sandstone packages of the Coal Cliff Sandstone (scale = 1.5 m; EPE = end-Permian extinction horizon). **(B)**, Detail of the Frazer Beach Member and its contacts (scale bar = 50 cm).

(commonly with a cobble-rich basal lag) of the Coal Cliff Sandstone. A supplementary reference section is represented in the EHKL-1 (Lisarow) well at 647.05–646.0 m, although it is possible that the base of the unit was removed from this core, along with the underlying Vales Point coal seam, for geotechnical analysis.

## Stratigraphic Hierarchy

In the type section, the FBM is designated the uppermost component of the Moon Island Beach Formation, constituting the uppermost part of the Newcastle Coal Measures, in turn representing the uppermost unit of the Singleton Supergroup. We also recognize the persistence of the FBM into the southern and western Sydney Basin, where it represents the uppermost unit of the Sydney Subgroup, within the Illawarra Coal Measures (**Figure 2B**).

## Lithology and Sedimentary Petrology

The FBM is dominated by shale and siltstone with few other lithologies (**Figures 3A–E**, **5E**,F,I). Locally, a <20-cm-thick discontinuous bed of organic-rich microbreccia or granulestone occurs at the base of the unit. This bed consists of massive or weakly stratified aggregations of silt- to granule-sized siliciclastic grains, organic detritus, and irregular to rounded pebble-sized clasts of probable pumice or reworked clay galls (**Figures 6A–F**). Becker et al. (2004), (supplementary figure S1) illustrated putative shocked quartz grains, representing c. 1% of the quartz fraction, from the microbreccia bed at Frazer Beach. However, our petrographic investigations of this layer at Frazer Beach, Snapper Point, and a stratigraphically equivalent bed in the GSQ Taroom 10 well in the Bowen Basin, did not yield any convincing examples of quartz grains with intersecting planar deformation features. Charcoal and angular reworked coal fragments are common in this basal bed (**Figures 6A,B,F**). Overlying this bed, and locally replacing it, is a succession, several decimeters to several meters thick, of medium to dark gray shale and siltstone that locally contains fine charcoal particles, degraded woody debris and fungal remains (Vajda et al., 2020, figures 5E,M). In some outcrops, fissility is poor, and the rocks are better described as mudstones that develop a blocky to conchoidal weathering pattern. The mudrocks typically become paler and may coarsen upward through the unit to include a few laminae of fine-grained sandstones near the top. Where no sharp-based sandstone rests directly upon this unit, the FBM has a gradational upper boundary and coarsens upward over several meters into thinly interbedded siltstone and sandstone (Facies Associations E/F: floodbasin deposits) or thinly bedded fine-grained sandstone (Facies Association D: levee deposits) of the Dooralong Shale Fielding et al. (2020).

The dominant sedimentary structures are flat or undulatory laminae. Diessel et al. (1967) noted that some layers are strongly fissile owing to alignment of plant debris and mica grains parallel to bedding. Current ripple cross-lamination with accessory wave-generated and combined-flow ripples are locally developed in the upper part of the unit. Diessel (1992 figure 6.10) illustrated dark

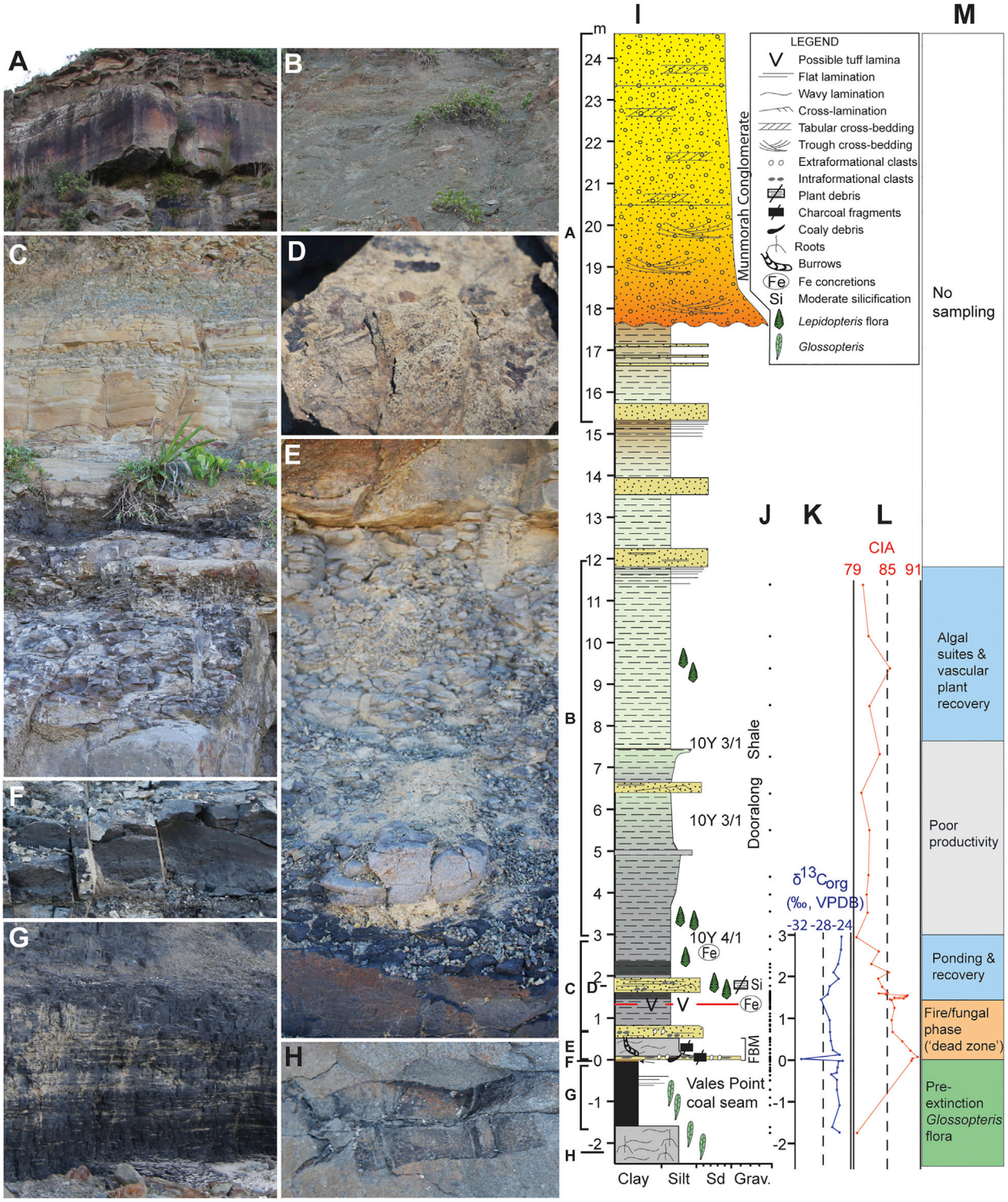


**FIGURE 5 |** Type section of the Frazer Beach Member with representative lithologies of this unit and its bounding strata. **(A)**, Cross-bedded sandstones of the basal Munmorah Conglomerate. **(B)**, Olive green siltstones of the upper Dooralong Shale. **(C)**, Siltstones and thinly laminated fine-grained sandstones of the lower Dooralong Shale. **(D)**, Plant debris dominated by *Lepidopteris callipteroides* on bedding plane of the lower Dooralong Shale. **(E)**, Siltstones of the Frazer Beach Member (incorporating a sand-filled vertebrate burrow above the basal microbreccia) overlain by basal sandstone of the Dooralong Shale. **(F)**, Basal microbreccia of the Frazer Beach Member. **(G)**, Vales Point coal seam. **(H)**, *Vertebraria* in paleosol underlying the Vales Point coal seam. **(I)**, Graphic log of coastal cliff (type section) at Frazer Beach. (FBM = Frazer Beach Member) **(J)**, Position of palynological samples studied by Vajda et al. (2020). **(K)**, $\delta^{13}C$ values for bulk organic material of the Vales Point coal seam, Frazer Beach Member and lower Dooralong Shale. **(L)**, Chemical Index of Alteration values for the interval from the Vales Point coal seam to upper Dooralong Shale. **(M)**, Dominant characteristics of palynological assemblages from the Vales Point coal seam to upper Dooralong Shale (after Vajda et al., 2020). For scale, the brackets in **Section 1** represent the stratigraphic coverage of the photographs in **(A–H)**; the fossil root in **(H)** is 15 mm wide. Mudrocks are gray colors unless otherwise noted by Munsell codes.

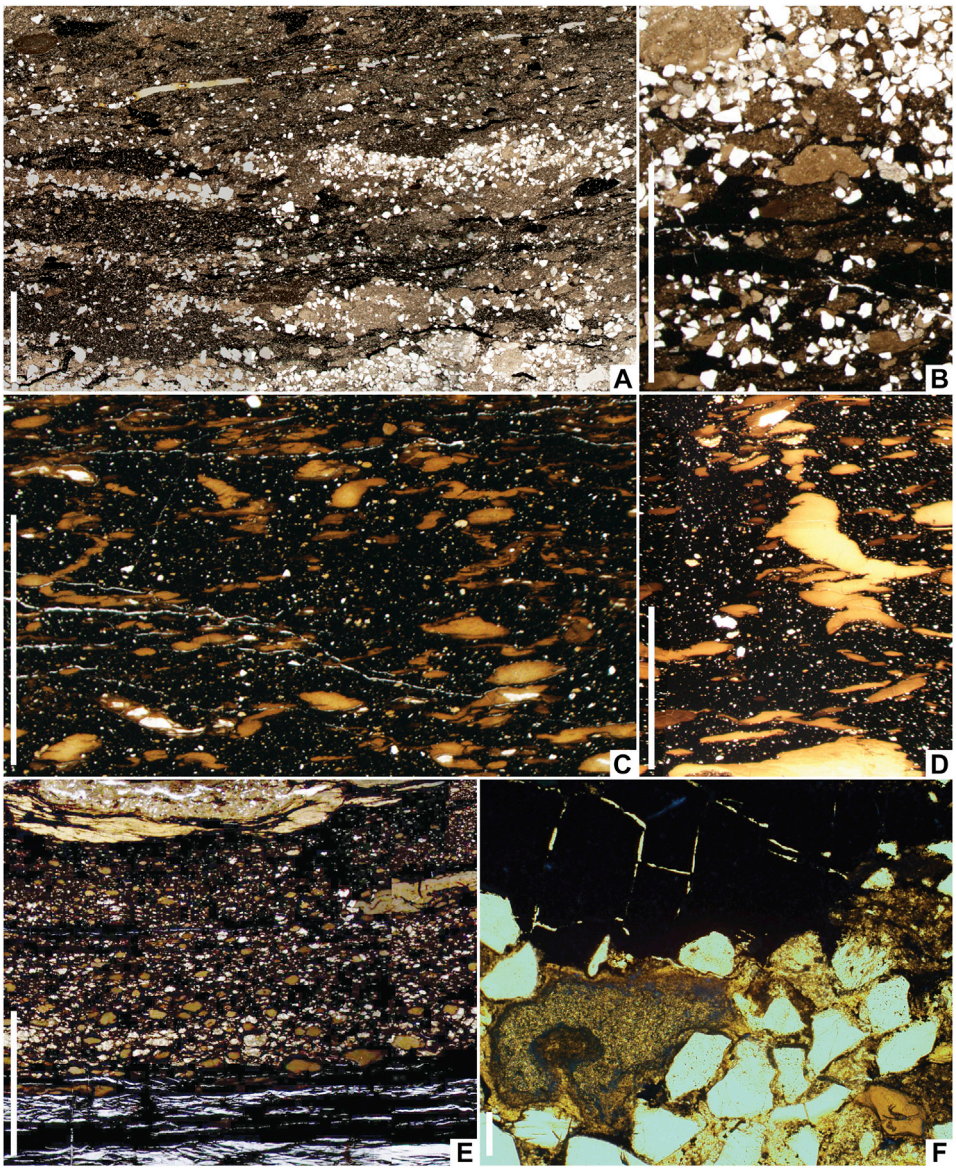


**FIGURE 6 |** Light (brightfield) micrographs of thin sections from the basal organic-rich granulestone/microbreccia of the Frazer Beach Member (Sydney Basin: **A–D**, **F**) and an equivalent bed at the base of the "marker mudstone" of the Bowen Basin **(E)**. **(A)**, Lenticular laminae of angular quartz grains, coal particles and clay pellets; type section, Frazer Beach. **(B)**, Enlargement of angular, monocrystalline, quartz grains, elongate coal fragments and angular to rounded clay pellets, type section; Frazer Beach. **(C)**, Organic-rich microbreccia dominated by angular and string-like masses of pumice fragments; Wybung Head. **(D)**, Large pumice clasts (equivalent to the "kaolinite worms" of Diessel et al. (1967) set in an organic-rich matrix; Snapper Point. **(E)**, Normally graded organic-rich sandstone–granulestone incorporating sporadic large pumice clasts at the base of the "marker mudstone" overlying the calcite-veined uppermost Permian coal in GSQ Taroom 10 borehole (212.7 cm depth). **(F)**, Enlargement of angular quartz grains, clay pellets, and cleated coal fragment set in a ferruginous cement; type section; Frazer Beach. Scale bars for **(A–E)** = 5 mm; **(F)** = 200 μm.

siltstone interlaminated with thin sandstones organized into asymmetrical to near-symmetrical ripples of 3–7 mm amplitude and around 44 mm wavelength from beds above the Bulli Coal in the southern Sydney Basin. Large, sand-filled mudcracks are relatively common in this unit in the southern Sydney Basin (Diessel et al., 1967, figure 4; Clark, 1992, figure 23). Synaeresis cracks and a low-diversity suite of bedding-parallel and facies-crossing trace fossils are present in some sections along the basin axis. In a few cores (especially near Wyong), a more diverse trace fossil suite including *Diplocraterion* and other facies-crossing traces is preserved (Fielding et al., 2020).

Apart from abundant clays, Diessel et al. (1967) noted that the mudrocks contain grains of quartz, feldspars, muscovite, and assorted heavy minerals. They also noted growths of fine siderite,

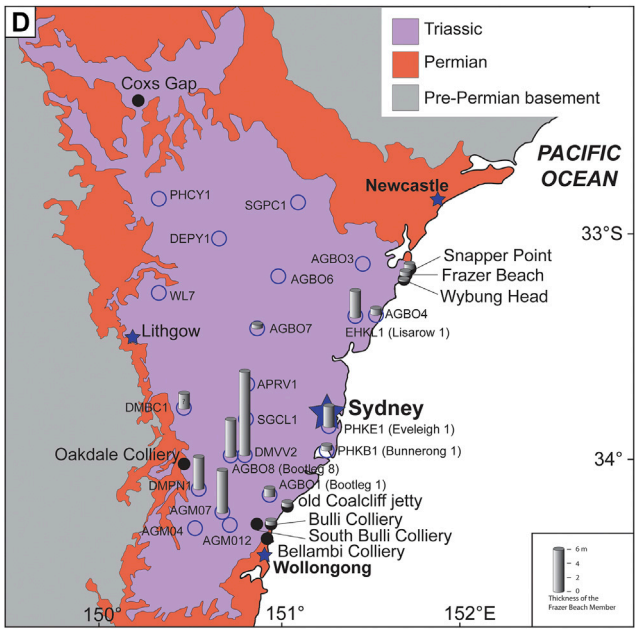


**FIGURE 7 |** Map of the Sydney Basin showing the interpreted thickness of the Frazer Beach Member, represented by vertical bars, in selected wells. Those wells without bars lack obvious representation of the Frazer Beach Member owing to erosional removal, faulting, analytical removal of core, non-deposition, or inadequate core data recovery.

calcite and dolomite crystals through the fabric of some poorly fissile shales. Locally, siderite accumulation is sufficient to form ironstone bands within the shales.

## Thickness

The unit is 50 cm thick in the type section (**Figures 3A–C**) but varies in thickness elsewhere in the basin (**Figure 7**). At Coalcliff, southern Sydney Basin, the FBM is 53 cm thick but the top of the unit is erosionally truncated by the Coal Cliff Sandstone. Isopachs of the "upper ply of the Bulli Coal" (**Figure 8A**) and Bulli Coal "roof shales" (**Figure 8B**) compiled by Clark (1992) and assigned to the FBM herein indicate thicknesses exceeding 5 m through the central part of the southern Sydney Basin.

## Lower Boundary

The lower boundary of the unit is defined as the gradational, sharp, or very slightly erosional contact between the Vales Point coal seam and its lateral equivalents (e.g., the Bulli Coal and Katoomba Coal Member) and the gray or black, weakly laminated shales and siltstones or basal granule-textured, dark gray microbeccia bed of the FBM. Vajda et al. (2020) noted prominent, laterally continuous, jarosite staining at the boundary between the underlying coal and the FBM at the type locality and neighboring sections. The lower boundary is commonly not preserved in exploration well cores owing to removal of the lowermost darker beds of the FBM together with the underlying Bulli Coal or Vales Point coal seam for destructive analysis.

## Upper Boundary

In the type section, the top of the FBM is defined by a sharp but conformable contact between medium-gray siltstones and a 30-cm-thick bed of massive fine-grained sandstone interpreted by Fielding et al. (2020) to represent a splay deposit at the base of the Dooralong Shale. In some boreholes (e.g., ELT Dooralong 8: Fielding et al., 2020; figure 14), the FBM has a gradational upper

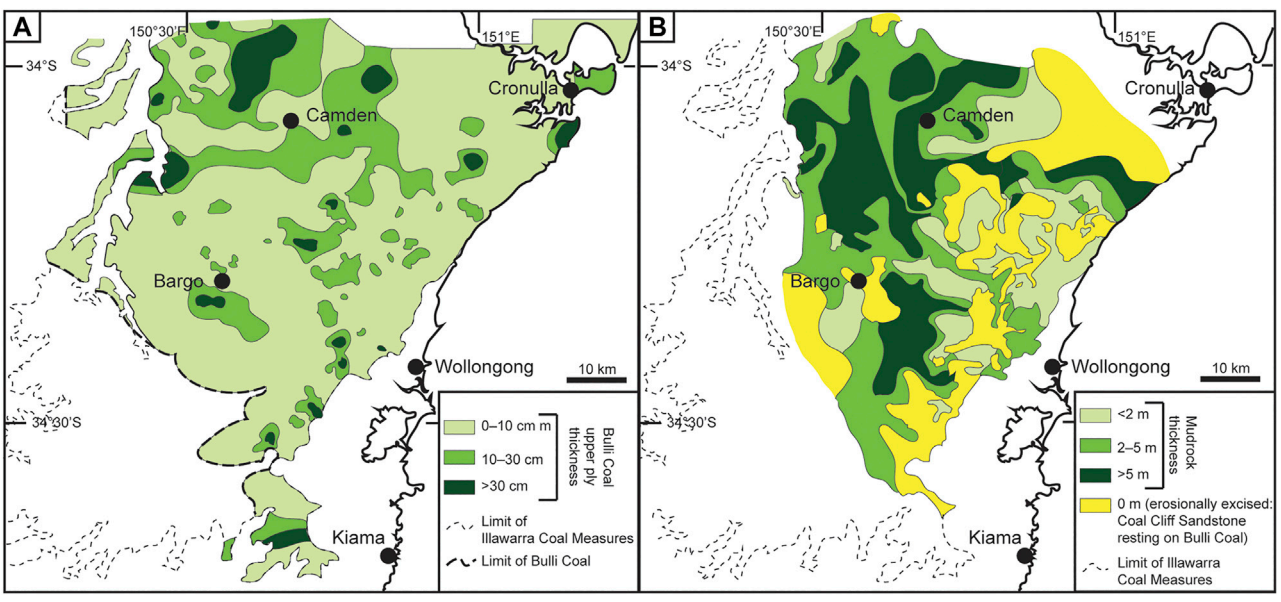


**FIGURE 8 |** Isopach maps showing the distribution of the Frazer Beach Member in the southern Sydney Basin. **(A)**, Isopach map of the basal organic-rich granulestone/microbreccia bed, also previously known as "the blacks" or the "upper transitional ply" of the Bulli Coal. **(B)**, Isopach map of the dominant mudrock component of the Frazer Beach Member. Maps adapted from Clark (1992).

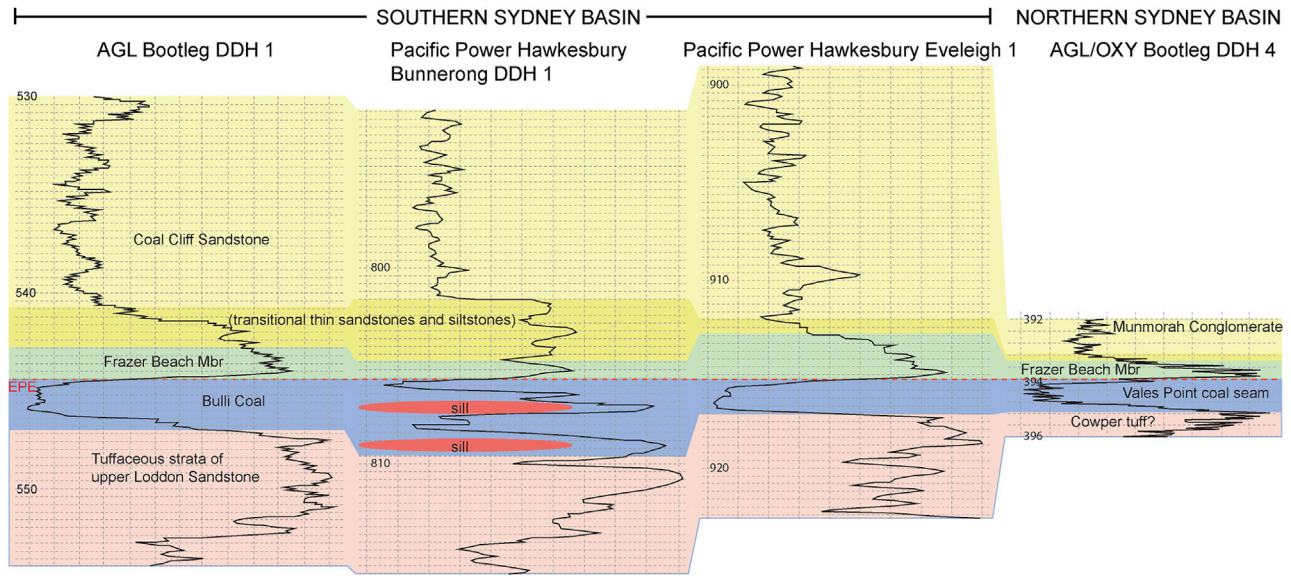


**FIGURE 9 |** Correlation of downhole gamma-ray logs spanning the Frazer Beach Member, uppermost Permian coal seam, and adjacent units between four wells in the Sydney Basin (well locations shown in **Figures 1**, **7**). Data derives from respective unpublished well completion reports held by the W.B. Clarke Geoscience Center drillcore library, Londonderry, New South Wales, Australia. Depths indicated in meters.

contact, passing upward into interlaminated fine-grained sandstones and medium-gray siltstones representative of the Dooralong Shale. Higher in the succession, the Dooralong Shale typically changes initially to mottled green–gray or blue–gray, then green–red shales and siltstones with increasing proportions of sandy beds near its upper contact with the Munmorah Conglomerate. In southern parts of the basin, the FBM is sharply (locally, erosionally) overlain by coarse-grained cross-bedded sandstones with pebbly lag layers characteristic of fluvial channel deposits (Coal Cliff Sandstone). In coastal exposures near Coalcliff, the upper part of the unit includes at least three discrete Fe-rich concretionary bands, each 1–4 cm thick. Where represented in the west of the basin, the FBM is overlain across an erosional contact by the Caley Formation or stratigraphically higher units.

## Gamma Ray Log Signature

The FBM has a distinctive gamma-ray signature in borehole geophysical logs. Gamma-ray values show an initial strong positive inflection following the consistently low values characterizing the underlying Bulli Coal and Vales Point coal seam (**Figure 9**). This may relate to the presence of tuffaceous material in the basal microbreccia of the FBM (Fielding et al., 2020). Values then decline in a stepwise manner upward through the remainder of the unit. The gamma-ray signal at the top of the FBM is variable. It ranges from a sharp decline to low values (e.g., where the unit is overlain abruptly by the Munmorah Conglomerate), to a more gradual reduction or fluctuating levels (e.g., where the unit is overlain by an interval of intercalated sandstones and siltstones: **Figure 9**). The succeeding sandstone- and conglomerate-dominated basal Narrabeen Group (Coal Cliff Sandstone and Munmorah Conglomerate) is characterized by consistently low gamma-ray values.

## Geochemical Signature

Stratigraphic profiles from various sites in the Sydney Basin show that the FBM records a transition in $\delta^{13}C_{org}$ values, from c. –24 to –26‰ in underlying strata (uppermost Permian coal seam and associated strata) to values of c. –25 to –27‰ in overlying Triassic strata (Dooralong Shale and equivalents: Fielding et al., 2019; Vajda et al., 2020; Mays et al., 2020). Based on data from the type locality and nearby Snapper Point, the FBM is characterized by $\delta^{13}C_{org}$ values averaging c. –26‰ (**Figure 5K**). However, samples immediately above the EPE horizon reveal excursions to very low values (c. –31‰ at 4 cm above the base of the FBM type section). Low values are also recorded in algae-rich mudrocks of the overlying Dooralong Shale (c. –28‰; Vajda et al., 2020, figure 3; **Figure 5K**). TOC values decrease upward through the FBM, from c. 6.5–7 wt% in the basal microbreccia to <0.5 wt% in the upper 10 cm. Low TOC levels persist into the overlying Dooralong Shale (Vajda et al., 2020, figure 3). The FBM is characterized by CIA values of 88–89 (**Figure 5L**). In a stratigraphic context, these results define a prominent short-term excursion to higher CIA values from the generally increasing trend from a long-term average of c. 70 in upper Permian strata to c. 80 in Triassic strata (Fielding et al., 2019).

## Distribution and Correlation with Australian Successions

The FBM is well exposed north of Sydney at Frazer Beach (**Figures 3A–C**, **5A–I**) and Snapper Point (**Figures 3D,E**). The unit is represented extensively in boreholes above the Vales Point coal seam throughout the northern Sydney Basin and is

recognized in the southern part of the basin in coastal cliff sections near Bulli and Coalcliff (**Figures 4A,B**). The unit is widely represented in boreholes through the center of the basin (e.g., in PHKB-1 and AGLB-8). Toward the western margin of the Sydney Basin, the FBM may be locally represented above the Katoomba Coal Member of the coal- and tuff-rich Farmers Creek Formation, Wallerawang Subgroup, Illawarra Coal Measures (Bembrick, 1983). It is possible that the lowermost mudrock interval of the Beauchamp Falls Shale Member (Caley Formation, Narrabeen Group) logged at Browns Gap near Lithgow (Bembrick, 1983) represents a local expression of the FBM. However, in most locations along the cratonic margin of the basin, the FBM and, in some cases, the underlying Katoomba Coal Member, has been removed by erosion resulting in Narrabeen Group sandstones resting with an erosional contact directly on lower beds of the Farmers Creek Formation.

The FBM appears to be absent from most of the contiguous Gunnedah Basin. As the Permian-Triassic succession is traced northwards from the Sydney Basin across the Liverpool Ranges into the Gunnedah Basin, the contact between the Black Jack Formation (Illawarra Coal Measures equivalent) and Digby Formation (basal Narrabeen Group equivalent) becomes progressively more erosional, with a significant proportion of upper Permian strata excised (McMinn, 1993; Xu and Ward, 1993). Similarly, a large proportion of the Lopingian coal measures has been eroded from the nose of the Lochinvar Anticline in the Hunter Valley, northern Sydney Basin (Harrington et al., 1989).

Further north, strata equivalent to the FBM have been recognized within depocenters of the western and northern Bowen Basin and contiguous Galilee Basin (Wheeler et al., 2020). (Metcalfe et al., 2015, figures 12, 17), illustrated a >5-m-thick shale–siltstone interval overlying the Lopingian Bandanna Formation in the Origin Energy Meeleebee-5 well in the southern Bowen Basin (expanded in **Figure 10**) that hosts a negative $\delta^{13}$C-isotope ($\delta^{13}C_{org}$) excursion similar to that recorded in the FBM. Various other wells in the Bowen and Galilee basins also intersect a siltstone-dominated interval above the topmost Permian coal that is lithologically and stratigraphically equivalent to the FBM and overlying Dooralong Shale (**Figure 10**). This interval, informally termed the "marker mudstone," was initially recognized at the Newlands coal mine in the northern Bowen Basin (Clare, 1985; Michaelsen et al., 2000) as a lacustrine carbonaceous mudstone unit at the interface of the Rangal Coal Measures (Permian) and Rewan Group (predominantly Triassic). There, the unit is 2–22.9 m thick and consists of laminated carbonaceous siltstone with varve-like features, sparse plant fragments, and *Botryococcus* (green algal) remains (Michaelsen et al., 2000). The unit also contains subordinate sheet-like sandstones identified as crevasse-splay deposits (Michaelsen et al., 2000).

The boundary between the "marker mudstone" and the underlying Newlands Rider 1 seam (Rangal Coal Measures) appears conformable, but is marked by a prominent negative $\delta^{13}C_{org}$ excursion (Hansen et al., 2000; Michaelsen, 2002). In the northern Bowen Basin, the "marker mudstone" is overlain conformably or disconformably by the sandstone- and green–red mudstone-dominated beds of the lower Rewan Group (Michaelsen et al., 2000). At the Isaac Plains coal mine, the "marker mudstone" is separated from the uppermost Permian coal seam (either the Leichhardt Seam or the Philips Rider) by a coarsening upwards shale to sandstone unit. This package of probable Permian strata has a sharp, planar contact with the "marker mudstone." In the Bowen Basin, the organic-rich microbreccia characterizing the base of the FBM has been detected only in the "marker mudstone" in the GSQ Taroom 10 well, Denison Trough (southwestern Bowen Basin; **Figure 6E**).

The "marker mudstone" has a sheet-like geometry traceable in mine exposures for over 17 km along strike (Michaelsen et al., 2000). A lithologically similar 2–15-m-thick unit caps the Rangal Coal Measures at Suttor Creek, 17 km south of Newlands (Matheson, 1990). Mapping of the "marker mudstone" in the Bowen Basin suggests it is laterally continuous along the basin's western margin (Sliwa et al., 2017) but variable (<2 m to >6 m) in thickness. The "marker mudstone" (**Figure 10**) appears to be a widely distributed, thin, mudrock-dominated unit, the lower part of which is laterally equivalent to the FBM and similar to it in its lacustrine depositional environment. Where the "marker mudstone" is very thick, the upper part, extending into the *Playfordiaspora crenulata* or *Protohaploxypinus microcorpus* zones, probably correlates with the Dooralong Shale. Lacustrine conditions developed extensively in the Sydney and Bowen basins following differential compaction of underlying peats (Michaelsen et al., 2000), base-level rise as a result of foreland loading (Sliwa et al., 2017), or a combination of base-level rise and significant disruption to the hydrological cycle as a result of the end-Permian extinction and regional deforestation (Vajda et al., 2020; Wheeler et al., 2020).

In the eastern part of the epicratonic Galilee Basin (GSQ Tambo 1-1A well: **Figure 10**), Wheeler et al. (2020) recognized a mudrock-dominated interval equated with the "marker mudstone" of the Bowen Basin that yielded palynofloras characterized by a shift from predominantly translucent phytoclasts (in the underlying Bandanna Formation) to opaque phytoclasts. This transition was accompanied by a relative increase in algal (especially *Botryococcus* and acanthomorph acritarchs) and fungal remains but impoverishment in vascular plant spores and pollen. These authors also recognized a low-magnitude negative $\delta^{13}C_{org}$ excursion within the "marker mudstone", mirroring the pattern in the FBM of the Sydney Basin. In the northern part of the Galilee Basin (GSQ Muttaburra 1, OEC Glue Pot Creek 1, and CRD Montani 1 wells), the "marker mudstone" appears to have been removed by erosion (Phillips et al., 2017; Phillips et al., 2018).

Westwards, in the contiguous Cooper Basin, Gray (2000) reported a >12-m-thick carbonaceous interval at the base of the mudstone- and siltstone-dominated Callamurra Member—the basal subunit of the Arrabury Formation, which rests on typical upper Permian coal-bearing successions of the Toolachee Formation (Draper, 2002). We suggest that at least part of this basal carbonaceous mudrock unit is coeval with, and depositionally akin to, the FBM.

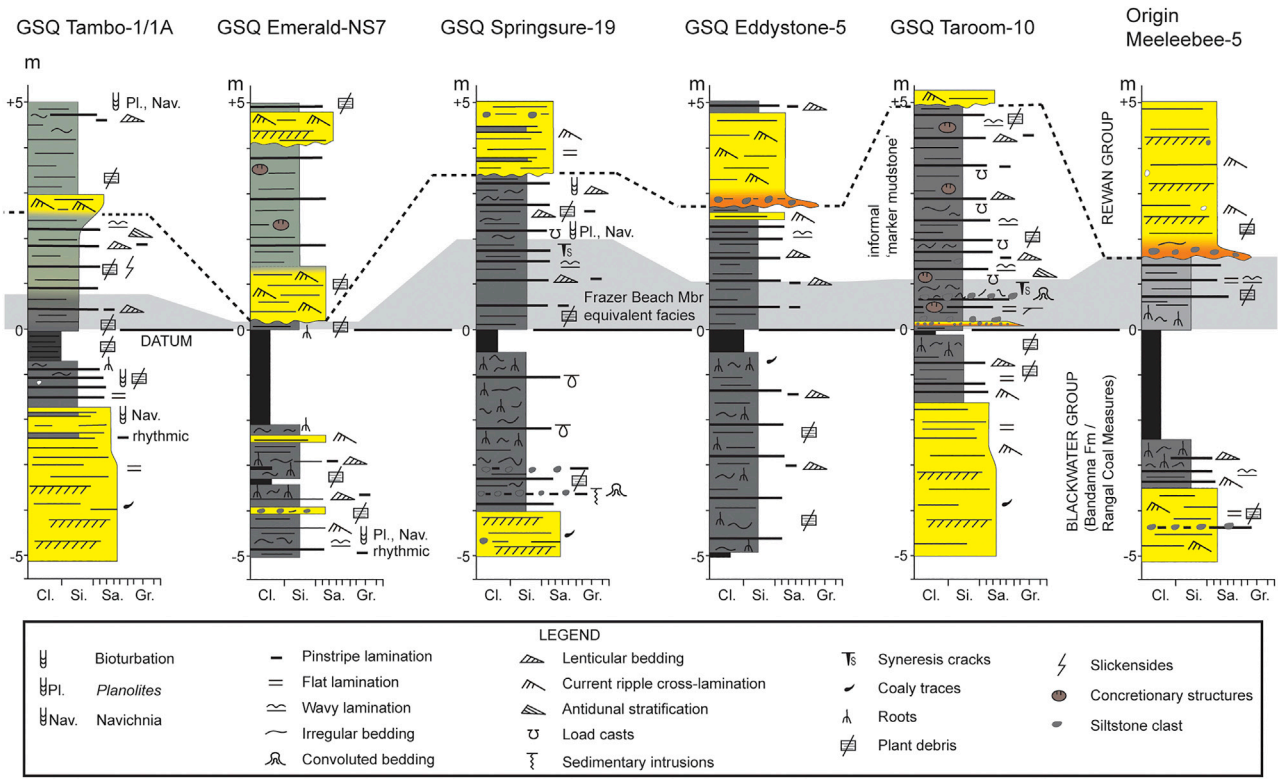


**FIGURE 10 |** Graphic logs of portions of six fully cored stratigraphic wells from the Galilee and Bowen Basin incorporating the "marker mudstone" overlying the uppermost Permian coal. The lower, organic-rich component, lacking complex sedimentary structures and trace fossil assemblages (shaded light gray), is interpreted as stratigraphically equivalent to the Frazer Beach Member of the Sydney Basin.

## Intercontinental Correlation

Spikes in the relative abundance of fungal and/or algal palynomorphs, dispersed charcoal, or other expressions of a palynological "dead zone", coupled with a negative $\delta^{13}C_{org}$ isotope excursion, in various other sections around the world (Looy et al., 2001; Lindström and McLoughlin, 2007; Vajda and McLoughlin, 2007; Schneebeli-Hermann and Bucher, 2015; Tewari et al., 2015; Vajda et al., 2020) are potentially useful criteria for identifying units correlative with the FBM. Several examples of thin intervals of fine-grained non-marine strata with these paleontological and geochemical features are known from other parts of Gondwana.

The most robust correlations are arguably with successions in the Transantarctic Mountains and Victoria Land, Antarctica. At Mt Crean, Victoria Land, a carbon isotope anomaly and the last occurrences of coal, *Glossopteris* and *Vertebraria* occur up to 12 m below the contact between Weller Coal Measures and the overlying Feather Conglomerate (Retallack and Krull, 1999; Retallack et al., 2005). At Graphite Peak, Transantarctic Mountains, the EPE is identified at the contact between the uppermost coal of the Buckley Formation and the overlying greenish-gray siltstones and buff sandstones of the Fremouw Formation. At both localities, the uppermost Permian coal is overlain successively by a microbreccia bed then either laminites or massive claystone reminiscent of the FBM in the Sydney Basin (Retallack, 2005). Elsewhere in the Transantarctic Mountains, e.g., at Collinson Ridge, the identification of *Glossopteris* several meters above the Buckley–Fremouw Formation contact suggests that this lithostratigraphic boundary and the EPE do not correspond in all places (Collinson et al., 2006). Erosion of the uppermost Permian coal in the Amery Group, Prince Charles Mountains, East Antarctica, may have removed any facies equivalent to the FBM in that region (McLoughlin et al., 1997).

Correlations with the well-studied Karoo Basin succession, South Africa, are hampered by scarce radiogenic-isotope ages and conflicting interpretations concerning the placements of the EPE and PTB (Smith and Ward, 2001; Gastaldo et al., 2005; Ward et al., 2005; Gastaldo et al., 2015; Neveling et al., 2016; Gastaldo et al., 2018; Gastaldo et al., 2020). Although mudrock-dominated intervals rich in fungal/algal fossils and vertebrate burrows are known from close to the EPE in the Karoo Basin (Retallack et al., 2003; Steiner et al., 2003; Gastaldo and Rolerson, 2008), precise correlation with the FBM is confounded by repetition of these mudrock facies through the Karoo Basin Permian-Triassic transition. Further north, laminated lacustrine fish beds (c. 30 m thick) of the middle member of the Majiya Chumvi Formation, Kenya, are bracketed by palynoassemblages that are correlated with the *Dulhuntyispora parvithola* and *Playfordiaspora cancellosa*

assemblage zones (Hankel, 1992), suggesting deposition coeval with the FBM and Dooralong Shale.

In the Iria rivulet of the Son-Mahanadi Basin complex of central India, a 1.5 m interval of shale and siltstone exposed at the base of the Panchet Formation conformably overlies the Changhsingian coal-bearing Raniganj Formation (Saxena et al., 2018, figure 3). This interval hosts the last convincing examples of *Glossopteris*, *Vertebraria* and *Schizoneura gondwanensis* in this basin, and also contains the lowermost examples of the typical Triassic plant *Dicroidium*. The presence of *Playfordiaspora* and high relative abundances of both glossopterid (*Striatopodocarpites*) and corystosperm (*Falcisporites*) pollen (Srivastava et al., 1997) suggests that this thin interval delineates the end-Permian floristic turnover and is probably correlative with the FBM.

## Depositional Setting

The laminated mudrocks of the FBM, assigned to facies association G by Fielding et al. (2020), are interpreted to represent the deposits of shallow lakes that developed in the aftermath of the EPE. The fine-grained lithologies, low-energy sedimentary structures, and facies stacking relationships signify deposition under standing-water conditions developed extensively following extinction of the lowland *Glossopteris* flora, cessation of peat development and continued subsidence of the peat surface (Vajda et al., 2020). The tabular sandstone overlying the FBM in the type section is interpreted to represent a splay deposit from nearby fluvial channels that spread across the shallow floodbasins during a minor flood event.

We find no evidence for marked aridification during deposition of the FBM but periodic desiccation of lake floors is evidenced by the development of large-scale mud cracks in lacustrine facies at Bulli Colliery (Diessel et al., 1967, figure 4) and sporadic tetrapod trackways and burrows in equivalent beds elsewhere in the basin (Harper, 1915; Retallack, 1996; McLoughlin et al., 2020). Isopach maps of the FBM indicate thicknesses of 2–5 m through central parts of the southern Sydney Basin (**Figures 8A,B**) indicating sediment accumulation in quiet waters over a broad region. Paleo-lake systems persisted during deposition of the Dooralong Shale in the northern Sydney Basin, but incorporated additional splay and levee deposits and are inferred to have experienced salinity or nutrient fluctuations and higher rates of desiccation based on stronger paleosol development (green, brown and red mottling) and variation in fossil algal suites (Retallack, 1999; Vajda et al., 2020).

Grebe (1970) reported abundant algae/acritarchs from the Dooralong Shale, which led subsequent authors to invoke a significant marine or brackish incursion into the Sydney Basin following collapse of the of the last Permian mire ecosystems (Helby, 1973; Bembrick, 1980; Retallack, 1980). Abundant algae have been reported from numerous sections through the upper FBM and lower Dooralong Shale (Hennelly, 1958; Mays et al., 2020; Vajda et al., 2020). However, most of these represent planktonic freshwater algae with affinities to Trebouxiophyceae (*Quadrisporites*) or Zygnematophyceae (*Brazilea*, *Circulisporites*, *Peltacystia*; Mays et al. (2021) and relate to extensive ponding on alluvial plains in the aftermath of the EPE (Vajda et al., 2020). Abundant leiospherid acritarchs (*Leiosphaeridia*) have also been reported from these strata (Vajda et al., 2020; Mays et al., 2021), but this group is polyphyletic (Moczydłowska and Willman, 2009) and the Sydney Basin forms are probably affiliated with non-marine Trebouxiophyceae (Mays et al., 2021). Only rare occurrences of coastal ichnofossils in cores near Wyong may indicate brief marine incursions into the basin depocenter (Fielding et al., 2020).

The black to dark gray, organic-rich granulestone–microbreccia bed, variably represented at the base of the FBM, is interpreted to represent primarily debris reworked from underlying strata. Retallack (2005) interpreted this bed to represent redeposited soils of contrasting composition at separate sites. The example at Coalcliff contains abundant coal and wood fragments from the underlying Bulli Coal and was termed a histic pedolith. The equivalent bed at Frazer Beach contains irregular clasts with highly birefringent streaks interpreted as aggregates (peds) from clayey Bt horizons of well-drained soils and was termed a sepic pedolith. Retallack (2005) suggested that such beds were generated by debris flows and mudflows. The microbreccia bed in the southern Sydney Basin documented by Retallack (2005) appears to equate with the upper ply of the Bulli Coal in earlier studies (Diessel et al., 1967). A 1–5-cm-thick claystone parting at the base of this ply was described by Diessel et al. (1967) as a dark brown to black pelletonstein containing small clasts of organic-stained allophane, micro- to cryptocrystalline kaolinite aggregates (called "worms"), and charcoal (semifusinite). Fielding et al. (2020) interpreted the high-birefringent pebbles from the microbreccia at Frazer Beach as altered pumice clasts. They considered such beds to be common above seams throughout the Newcastle and Illawarra coal measures, and represented deposits of local erosion potentially triggered by ash showers from distant volcanic eruptions based on texturally similar deposits elsewhere (Jorgensen and Fielding 1996, figure 4; Yago and Fielding 2015, figure 7F). Each interpretation emphasized a brief pulse of erosion at the base of the FBM in the immediate aftermath of peat forest denudation during the EPE.

In the northern Bowen Basin, the coeval "marker mudstone" is also interpreted to have been deposited in large floodbasin lakes based on its sheet-like geometry, predominantly fine-grained lithology, varve-like laminae, sparse *Planolites* trails, and *Botryococcus* remains (Michaelsen et al., 2000). Also equivalent to the FBM is the presence of a texturally similar, thin, dark granulestone–microbreccia bed at the base of the "marker mudstone" in GSQ Taroom 10 in the southwestern Bowen Basin (**Figure 6E**).

We exclude a sharp change in the regional tectonic regime as a primary influence on accumulation of the FBM owing to the distribution of this thin unit and its correlatives over a substantial distance (thousands of km) in various basins of contrasting tectonic and geodynamic context (both foreland and epicratonic basins) in eastern Australia. Moreover, the timeframe for deposition of this unit spans only a few thousand years—an interval that is probably too brief for

tectonism to influence sedimentation over such a wide area. Tectonism can influence drainage patterns and sediment sources but our provenance data (palaeocurrents, elemental ratios and sandstone petrography: Vajda et al., 2020; Fielding et al. 2020) show no evidence for a major shift in sediment dispersal through this interval. The number and thickness of tuff beds in the Sydney and Bowen basins, indicative of mountain building in the New England Orogen, wanes through the Permian–Triassic transition suggesting comparatively subdued tectonism through this interval. The inter-regional extent of the FBM suggests its genesis is unrelated to any process confined to individual basins.

### Geotechnical Significance

The FBM constitutes the roof strata of several coal mines exploiting the uppermost Permian seam—most notably the Bulli Coal in the southern Sydney Basin. Diessel and Moelle (1965) outlined various issues relating to stability of these strata in coal workings. In particular, they noted that rocks of the FBM form a roof of fair stability where: 1) they lack structural disturbance; 2) abrupt facies changes are not represented; 3) a clean parting separates these strata from the underlying coal seam; 4) organic laminae do not form weaknesses in the bed fabric; and 5) the thickness of the lowermost bed exceeds 25 cm.

These stability criteria are not always met in the Sydney Basin mines and roof collapse has commonly been associated with major gas outbursts from the Bulli Coal (Harvey and Singh, 1998). Thin lamination, micaceous and organic partings, and low cohesive strength (especially near structural discontinuities) of the FBM strata pose ongoing challenges for mining operations. Such hazards are highlighted by at least 11 fatalities recorded from individual rock falls from the roof or working face or from collapse of support structures in the Bulli Colliery alone between 1861 and 1987 (Illawarra Coal, 2020).

## AGE CONSTRAINTS ON THE FRAZER BEACH MEMBER USING CA-IDTIMS

### Dating the End-Permian Extinction and Permian-Triassic Boundary

The Permian–Triassic boundary, as defined by the first appearance datum of the conodont *Hindeodus parvus* from about the middle of bed 27 of the GSSP section at Meishan, China, is dated as 251.902 ± 0.024 Ma (Burgess et al., 2014). This date is a mathematical construct obtained from high-precision CA-IDTIMS analyses of two successive ash beds (beds 25 and 28) in the stratotype section. Bed 25 was dated as 251.941 ± 0.037 Ma and bed 28 as 251.880 ± 0.031 Ma, both from presumed ash-fall zircons (Burgess et al., 2014). The ash beds are separated by the 22 cm spanning beds 26 and 27. The marine extinction interval initiates at bed 25 and persists to bed 28, representing a time duration of 61 ± 46 kyr (Burgess et al., 2014). This represents an average sedimentation rate of 0.36 cm/kyr (with a potential range of 0.21–1.47 cm/kr) at Meishan.

### Dating the Sydney Basin Succession

Historically, the default placement of the PTB in the Sydney Basin has been at the top of the uppermost coal seam (Bulli Coal in the south, Katoomba Coal Member in the west, and Vales Point coal seam in the northeast: David, 1950; Hutton and Bamberry 1999; Ives et al., 1999). Radiogenic isotope ages, palynological data, and carbon isotope profiles (Fielding et al., 2019; Fielding et al., 2020; Mays et al., 2020; this study) indicate that the PTB is somewhat higher than the top of the uppermost coal and above the overlying FBM.

Here we summarize recent CA-IDTIMS data from tuffs and ash-bearing siliciclastic beds that constrain the ages of the FBM, the EPE, and the PTB in the Sydney Basin (**Table 1**; **Figure 11**). All radiogenic age estimation was undertaken on euhedral zircon crystals to avoid the chances of analyzing reworked examples. Where these crystals derive from discrete tuff layers, the obtained dates are assumed to correspond closely to the depositional age of the beds. Where they derive from grains extracted from fine-grained siliciclastic layers, the obtained dates represent maximum depositional ages. Fifteen samples analyzed by CA-IDTIMS are key to constraining the age of the FBM and the major events around the end of the Permian (**Figure 11**).

The key outcomes of this high-resolution dating are:

(1) Samples GA2666257–258, GA2666255, GA2055445, and GA2152418 yield consistently younger ages with stratigraphic position providing a strong measure of confidence for estimating sedimentation rates through the Changhsingian interval of the northern Sydney Basin (see sedimentation rate calculations of Mays et al., 2020).
(2) Sample GA2055445 (252.70 ± 0.05 Ma) derives from a tuff directly beneath the Wallarah coal—the seam stratigraphically beneath the Vales Point coal. In some places, the Wallarah and Vales Point seams amalgamate Fielding et al. (2020), hence the underlying tuff provides a maximum temporal constraint on the last phase of coal accumulation in the northern Sydney Basin.
(3) Sample GA2152418 (252.64 ± 0.07 Ma) derives from a tuff overlying the Wallarah coal seam and is dated to c. 60 kyrs younger than the preceding sample from below this coal seam. The date confirms a late Changhsingian age for the upper part of the Newcastle Coal Measures and provides a measure of the temporal span of peat accumulation represented by a typical Sydney Basin bituminous coal seam of average thickness.
(4) Samples GA3081568 and GA2152420 from the Moon Island Beach Formation in the northern Sydney Basin yielded ages that are markedly greater than those obtained from underlying samples and probably represent reworked zircon grains.
(5) Sample GA2127413 (252.60 ± 0.04 Ma) from a tuff low within the Bulli Coal and GA3081569 (252.10 ± 0.06 Ma) from the basal FBM provide age constraints on the accumulation of the uppermost Permian coal seam (c. 50,000 years) and suggest that the terrestrial EPE (at the

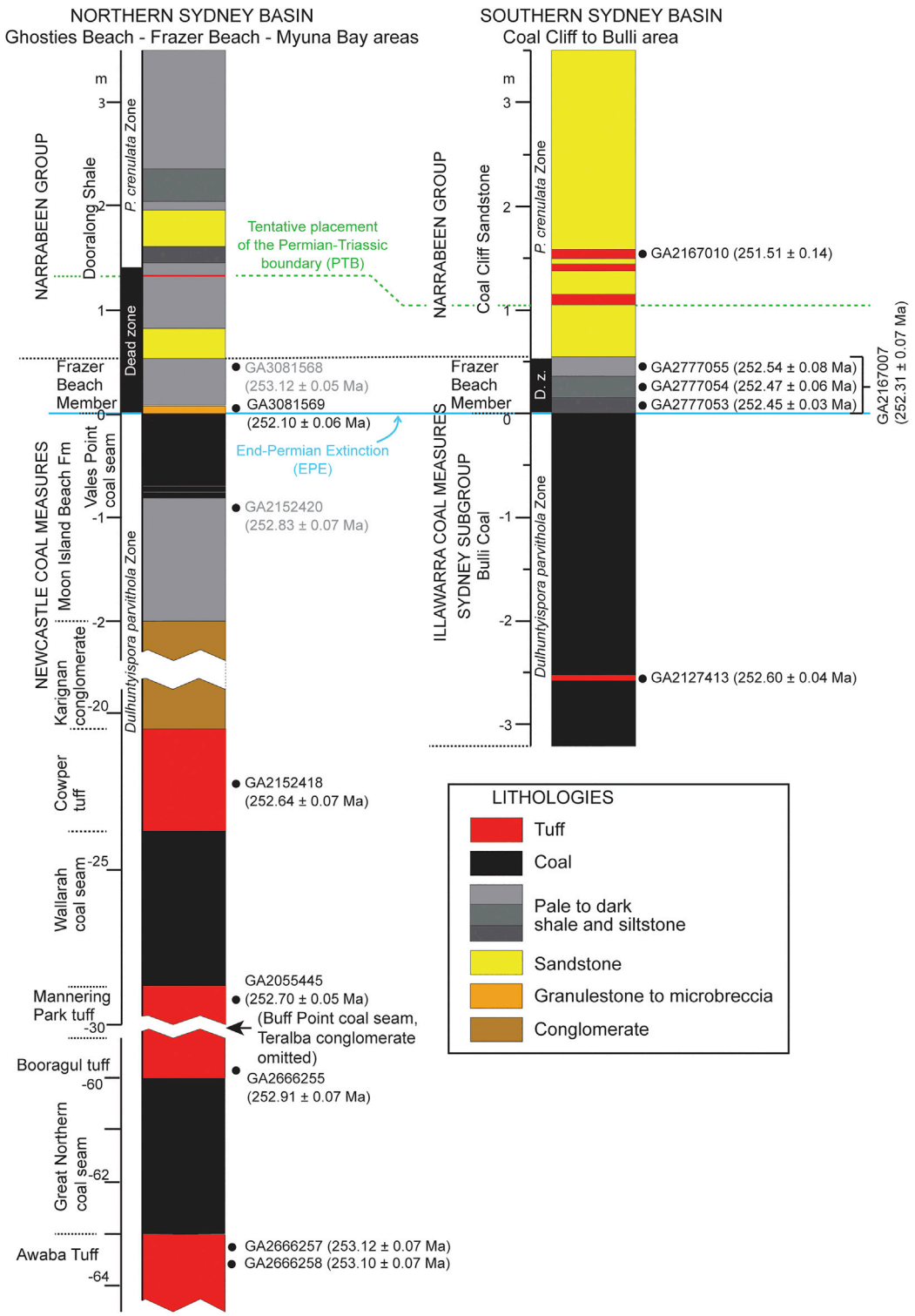


**FIGURE 11 |** Summary diagram of radiogenic-isotope dating results from CA-IDTIMS analysis zircons from uppermost Permian and lowermost Triassic tuffs in the Sydney Basin.

**TABLE 1 |** Summary of key ages from CA-IDTIMS dating of zircon grains obtained from tuffs and ash-bearing siliciclastic beds between the Awaba Tuff and the basal Narrabeen Group in the Sydney Basin, Australia. Details of individual grain ages, U-Pb isotopic data and measures of uncertainty are provided by Metcalfe et al. (2015), Fielding et al. (2019), and Fielding et al. (2020).

| Sample | Geographic source | Stratigraphic source | Age (CA-IDTIMS, unless otherwise stated) | References and comments |
|---|---|---|---|---|
| GA2167010 | Coal Cliff outcrop | Tuff or tuffaceous siltstone at 97–105 cm above the base of the Coal Cliff Sandstone (or 150–158 cm above the top of the Bulli coal) | Ages of 251.60 ± 0.19 and 251.38 ± 0.22 Ma obtained from two halves of a single grain (mean = 251.51 ± 0.14 Ma) | Fielding et al. (2020). This zircon is interpreted as being detrital based on morphology. The dating is considered to provide a maximum depositional age |
| GA3081568 | Snapper Point outcrop | 1.5 m above the Vales Point coal seam in the basal Dooralong Shale | Three grains yielded equivalent dates with a weighted mean of 253.12 ± 0.05 Ma | Fielding et al. (2020). Grains interpreted as being detrital given their rounding |
| GA2167007 | From under the Sea Cliff Bridge near the old mine entrance at Coalcliff | Bulk siltstone sample of the Frazer Beach Member from 0 to 53 cm above the Bulli Coal | 252.31 ± 0.07 Ma (based on a weighted mean of nine CA-IDTIMS analyses | Fielding et al. (2019) and Fielding et al. (2020). This sample represents a composite of the more narrowly delimited samples GA2777053–GA2777055 |
| GA2777055 | Under the Sea Cliff Bridge near the old mine entrance at Coalcliff | Siltstone at the top of the Frazer Beach Member at 36–53 cm above the Bulli Coal | 252.54 ± 0.08 Ma, based on a weighted mean of three of five CA-IDTIMS analyses. One of the others provided a younger age of 252.17 ± 0.13 Ma | Fielding et al. (2020) |
| GA2777054 | Under the Sea Cliff Bridge near the old mine entrance at Coalcliff | Siltstone in the middle of the Frazer Beach Member at 13–36 cm above the Bulli Coal | 252.47 ± 0.06 Ma (based on a weighted mean of four CA-IDTIMS analyses) | Fielding et al. (2020) |
| GA2777053 | Under the Sea Cliff Bridge near the old mine entrance at Coalcliff | Siltstone at the base of the Frazer Beach Member at 0–13 cm above the Bulli Coal | 252.45 ± 0.03 Ma (based on a weighted mean of seven CA-IDTIMS analyses) | Fielding et al. (2020). |
| GA3081569 | Frazer Beach | Microbreccia bed, 0–10 cm above base of Frazer Beach Member | Ages of 252.11 ± 0.08 and 252.08 ± 0.09 Ma obtained from two halves of a single grain, with a weighted mean of 252.10 ± 0.06 Ma | Fielding et al. (2020). Grain is interpreted as detrital given its morphology, hence its dating is considered to represent a maximum depositional age |
| GA2127413 | Underground exposures of the Metropolitan Colliery near Bulli | 1–2-cm-thick tuff located 0.61 m above the base of the 3.25-m-thick Bulli Coal | 252.60 ± 0.04 Ma | Metcalfe et al. (2015), Fielding et al. (2019) |
| GA3081568 | Snapper Point | Directly above the Vales Point coal seam | Three whole grains with a weighted mean age of 253.12 ± 0.05 Ma | Fielding et al. (2020). Because this age is greater than that of GA3081569 located in a similar stratigraphic position, and greater than samples from the stratigraphically lower units, we suggest that the dated zircons from this sample are reworked |
| GA2152420 | Ghosties Beach | Tuffaceous siltstone just below the Vales Point coal seam | 252.83 ± 0.07 Ma based on a weighted mean of six of the nine analyzed grains | Fielding et al. (2020). One of the grains yielded an outlier age of 251.44 ± 0.16 Ma, a result considered to be influenced by Pb loss |
| GA2152418 | Ghosties Beach outcrop | Cowper Tuff | 252.64 ± 0.07 Ma based on the weighted mean of six of seven analyses | Metcalfe et al. (2015). One younger date of 251.76 ± 0.16 Ma derives from a zircon grain that was probably subject to some Pb loss |
| GA2055445 | Myuna DDH 45 well at 0.70–1.70 m in the Centennial Coal | Above the base of the Mannering Park Tuff | 252.70 ± 0.05 Ma | Metcalfe et al. (2015). The age represents a weighted mean of the eight youngest dates. One older date of 340.10 ± 1.14 Ma was recovered for a recycled zircon grain |
| GA2666255 | Myuna coal mine, panel 511 easting 368388, northing 6340445 | Booragul tuff, 0–20 cm above Great Northern coal seam | 252.91 ± 0.07 Ma | Lowermost sample dated from Moon Island Beach Formation; The age is likely very close to the time of eruption and emplacement of the Booragul tuff |
| GA2666257 | Myuna coal mine, panel 511 easting 368388, northing 6340445 | Awaba Tuff (uppermost 10 cm) | 253.12 ± 0.07 Ma | The Awaba Tuff potentially represents a composite eruptive phase. The obtained age is likely very close to the time of eruption |
| GA2666258 | Myuna coal mine, panel 511 easting 368388, northing 6340445 | Awaba Tuff (10–40 cm below top of unit) | 253.10 ± 0.07 Ma | As above |

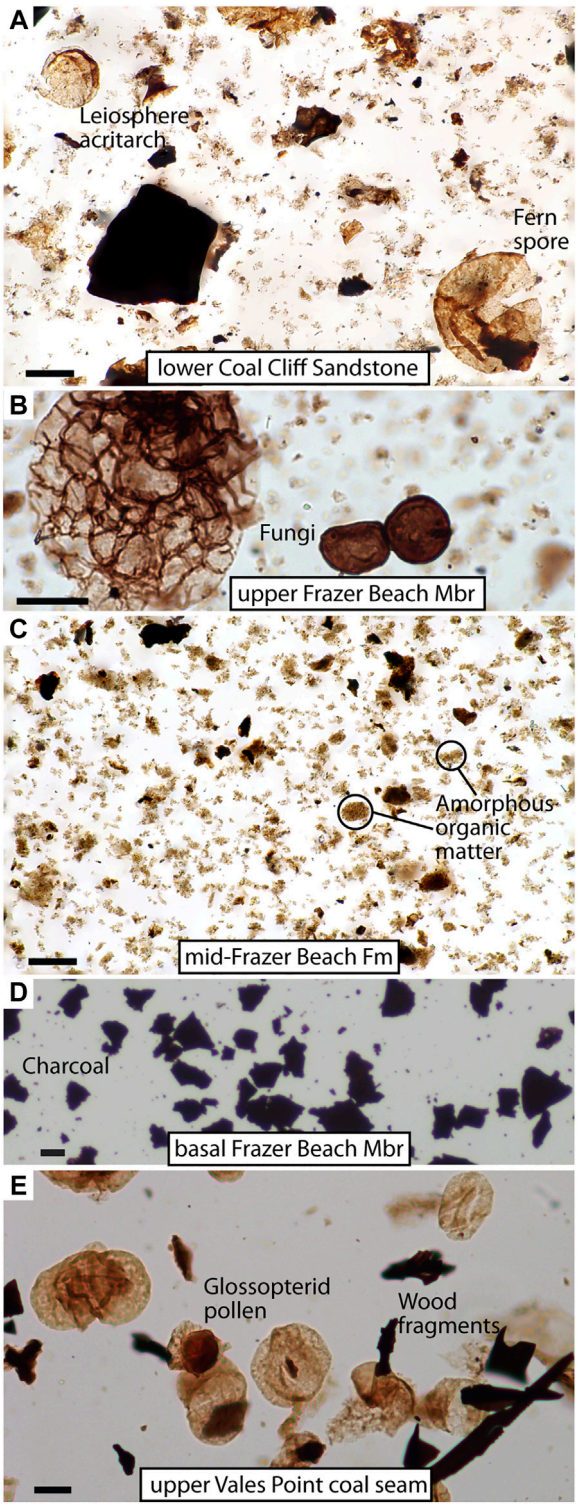


**FIGURE 12 |** Typical palynofacies from below, within and above the Frazer Beach Member, Sydney Basin; all scale bars = 20 μm. **(A)**, Post-extinction recovery flora of algae and fern spores, 310–320 cm above EPE (basal Coalcliff Sandstone), Coal Cliff. **(B)**, Fungal remains; Snapper Point, 53–56 cm above EPE (upper Frazer Beach Member). **(C)**, Kerogen assemblage rich in bacteria-derived amorphous organic matter; Coal Cliff, (*Continued*)

Vales Point coal seam to FBM contact) in eastern Australia is between c. 700 and 200 kyrs older than the PTB based on dating of the GSSP section at Meishan, China.

(6) Zircons from the FBM at Coal Cliff yield dates of 252.31 ± 0.07 Ma to 252.54 ± 0.08 Ma (**Figure 11**) implying the EPE in that area is >410–640 kyrs earlier than the PTB (depending on the veracity of the CA-IDTIMS dates, i.e., no reworking of grains or Pb loss from the crystals). Given that the succession of dates for samples GA2777053–2777055 is slightly out of geochronological order, some reworking of zircon grains may have occurred in these beds. The younger date of GA3081569 (252.10 ± 0.06 Ma), recovered from the basal microbreccia bed of the FBM in the northern Sydney Basin, is likely to be close to the age of the terrestrial EPE in eastern Australia if there has been no erosional removal of strata at the base of the type section. Collectively, these dates suggest that the terrestrial EPE in eastern Australia occurred at least 160 kyrs before the onset of the tropical marine extinction as dated in the Global Stratotype Section at Meishan (Burgess et al., 2014). No high-resolution dates are yet available for the marine extinction at high southern palaeolatitudes.

(7) Samples GA3081569 (252.10 ± 0.06 Ma) and GA2167010 (251.51 ± 0.14) from the FBM and Coal Cliff Sandstone, respectively, provide dates bracketing the top of the FBM, and also constrain the PTB to a position between the basal FBM and 1 m above the base of the Narrabeen Group.

## FOSSIL CONTENT

### Palynoflora of the Frazer Beach Member

The uppermost Permian coals of the Sydney Basin host palynofloras dominated by glossopterid pollen and diverse pteridophyte spores (**Figure 12E**). The contact between the Vales Point coal seam (and equivalent uppermost coals of the Sydney Basin) and the succeeding FBM corresponds to the boundary between the *Dulhuntyispora parvithola* Zone (Foster, 1982; Mantle et al., 2010; Mays et al., 2020), or the APP5 zone (Price, 1997), and the overlying "dead zone" of Vajda et al. (2020). This boundary corresponds to the extinction of the *Glossopteris* flora and is the expression of the terrestrial EPE in Gondwana. In the type section, the FBM is entirely within the "dead zone" of Vajda et al. (2020), a 140-cm-thick interval characterized by a depauperate palynoflora. The palynofacies characterizing the lowermost 34 cm of the unit is dominated by charcoal and opaque wood fragments (**Figure 12D**), with extremely sparse algal microfossils. Above this, the upper portion of the unit expresses an increase in amorphous organic matter (**Figure 12C**), probably representing enhanced algal and/or

**FIGURE 12** | 10–20 cm above EPE (middle Frazer Beach Member). **(D)**, Charcoal-dominated assemblage; Frazer Beach (type section), 0–8 cm above EPE (basal Frazer Beach Member). **(E)**, Typical palynoassemblage from uppermost Permian coal dominated by glossopterid pollen; Snapper Point, 4–5 cm below the EPE (Vales Point coal seam).

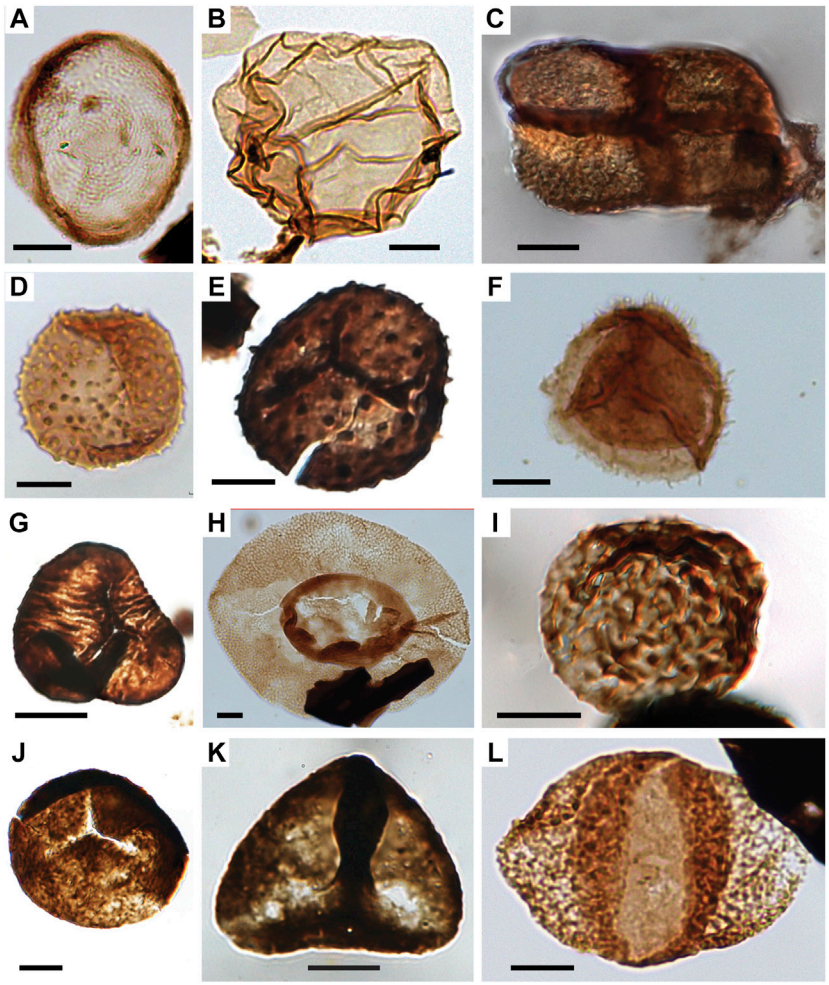


**FIGURE 13 |** Palynomorphs typical of the Frazer Beach Member and immediately adjacent strata, Sydney Basin, all scale bars = 10 μm, England Finder coordinates in parentheses. **(A)**, *Circulisporites parvus* de Jersey, 1962, Frazer Beach, 146–150 cm above EPE (basal Dooralong Shale), S200868 (L19/4). **(B)**, *Leiosphaeridia* sp., Frazer Beach, 144–146 cm above EPE (basal Dooralong Shale), S200870 (W44). **(C)**, *Quadrisporites horridus* Hennelly, 1958 emend. Potonié and Lele, 1961, Frazer Beach, 153–155 cm above EPE (basal Dooralong Shale), S200864 (X32/3). **(D,E)**, *Brevitriletes bulliensis* (Helby, 1970 ex; de Jersey, 1979) de Jersey and Raine, 1990; **(D)**, Frazer Beach, 148–150 cm above EPE (lower Dooralong Shale), S200868 (M20); **(E)**, PHKB-1, 801.11 m (4 m above EPE; Frazer Beach Member), S014103/2 (S46/3). **(F)**, *Krauselisporites* sp. Frazer Beach, 153–155 cm above EPE (lower Dooralong Shale), S200864 (M17). **(G)**, *Triplexisporites playfordii* (de Jersey and Hamilton, 1967) Foster, 1979, PHKB-1, 805.03 m (7 cm above EPE; Frazer Beach Member), S014101/1 (G42). **(H)**, *Playfordiaspora crenulata* (Wilson) Foster, 1979, Frazer Beach, 153–155 cm above EPE (lower Dooralong Shale), S200864 (Q29). **(I)**, *Thymospora ipsviciensis* (de Jersey) Jain, 1968, Coalcliff, 40–45 cm above EPE (Frazer Beach Member), S029710/3 (P18/4). **(J)**, *Cyclogranisporites gondwanensis* Bharadwaj and Salujha, 1964, PHKB-1, 805.03 m (7 cm above EPE; Frazer Beach Member), S014101/2 (K17/4). **(K)**, *Leiotriletes directus* Balme and Hennelly, 1956, PHKB-1, 805.03 m (7 cm above EPE; Frazer Beach Member), S014101/2 (F44). **(L)**, *Alisporites (Falcisporites) australis* de Jersey, 1962, Frazer Beach, 148–150 cm above EPE (basal Dooralong Shale), S200868 (B/20).

bacterial accumulation (Batten, 1996; Pacton et al., 2011), and a marked increase in fungal microfossils (**Figure 12B**). The first significant recovery of vascular plant spores and pollen is evidenced around 1.5 m above the base of the FBM in the type section (Vajda et al., 2020; **Figure 12A**).

The palynological record of the FBM in the southern Sydney Basin has a similar signature to the type section. At Coalcliff, the palyno-assemblages equivalent to the "dead zone" observed at Frazer Beach are dominated by high abundances of amorphous organic matter and wood fragments, with a modest up-succession increase in algal and plant microfossil abundance and diversity. They differ only in the absence of fungi. From Appin Bore 4, southern Sydney Basin, Hennelly (1958) reported a palynological "transition interval" characterized by poor palynomorph recovery but relatively high abundances of the alga *Quadrisporites horridus* (**Figure 13C**) in the initial 38 cm above the Bulli Coal, which likely corresponds to the FBM.

In the southern (Coalcliff, CCC-27) and central (PHKB-1) Sydney Basin, the palynoassemblages from plant-bearing beds of the upper FBM or overlying basal Coal Cliff Sandstone (Facies F of Fielding et al., 2020) are attributable to the *Playfordiaspora crenulata* Zone (upper Changhsingian–Griesbachian), indicated by the first occurrences of *Brevitriletes bulliensis* (**Figures 13D,E**) and/or *Triplexisporites playfordii* (**Figures 13F,G**; Hennelly, 1958;

Fielding et al., 2020; Mays et al., 2020). From Elecom Newvale DDH 28, northern Sydney Basin, Helby (1970) reported the first basin-wide occurrences of 17 palynomorph taxa in beds c. 33 cm above the top of the Vales Point coal seam, including the *P. crenulata* Zone index species mentioned above. These beds are probably attributable to the upper FBM or basal Dooralong Shale. The base of this zone is accompanied by increases in freshwater algae (*Q. horridus*), leiospherid acritarchs (**Figures 13A,B**) and fern spores (e.g., *Brevitriletes*, *Cyclogranisporites*, *Leiotriletes*, *Thymospora*; **Figures 13H–K**). Although the pollen records of the underlying Newcastle Coal Measures are dominated by taeniate bisaccate grains typical of glossopterids (*Protohaploxypinus*, *Striatopodocarpites*; **Figure 12E**), the dominant pollen of the strata succeeding the FBM are non-taeniate bisaccate forms [*Alisporites* (*Falcisporites*), *Pteruchipollenites*; **Figure 13L**].

## Palynoflora of the "Marker Mudstone" (Bowen Basin)

Palynological assemblages from the relatively thick (22.9 m) "marker mudstone" at the Newlands Coal Mine are referable to Price's (1997) APP6 zone (equivalent to the collective *Playfordiaspora crenulata* and *Protohaploxypinus microcorpus* zones) based on the appearance of *P. crenulata* (Michaelsen, 1999). This unit is also rich in *Botryococcus* (Trebouxiophyceae) at Newlands (Michaelsen et al., 1999). The APT1 zone (equivalent to the lower *Lunatisporites pellucidus* Zone) begins immediately above the mudstone.

The "marker mudstone" is much thinner (2–4 m) at the Isaac Plains coal mine than at Newlands but the palynological assemblages are similar (Wheeler, 2020). Samples collected from shale directly overlying the uppermost Permian coal seam, from the more expanded mudrock interval referred to the "marker mudstone", and from the siltstones of the overlying basal Rewan Group at Isaac Plains all yield taxa typical of the *Playfordiaspora crenulata* and *Protohaploxypinus microcorpus* zones (Wheeler, 2020). The most common index taxon is *Triplexisporites playfordii*; occurrences of *Playfordiaspora crenulata* are sparse. Other notable taxa typical of the *P. crenulata* Zone include *Thymospora ipsviciensis* and *Brevitriletes bulliensis*. Very rare specimens of *Reduviasporonites chalastus* are present. Bisaccate pollen grains, such as *Alisporites* (*Falcisporites*) *australis*, are very rare but increase in overlying strata. *Protohaploxypinus microcorpus* and *Lunatisporites pellucidus* were not observed. Cavate trilete spores of lycopsids, e.g., *Lundbladispora* spp., *Rewanispora foveolata* (an index taxon of the *P. microcorpus* Zone), and *Densoisporites playfordii* are common. Other common trilete spores include *Calamospora* sp., *Microbaculispora* spp. and *Leiotriletes directus*. The presence of rare pollen of Permian aspect (e.g., some *Protohaploxypinus* and *Striatopodocarpites* species) may indicate limited reworking of grains, or the production of taeniate pollen by some non-glossopterid groups in the post-EPE flora (Mays et al., 2020). Although a palynological "dead zone" was not detected in the Bowen Basin, the "marker mudstone" of that region correlates collectively with the FBM and overlying Dooralong Shale. The abundance of taeniate bisaccate (glossopterid) pollen in palynological samples recovered from the carbonaceous mudstones immediately below the Rewan Group in the Galilee Basin by Wheeler et al. (2020) suggests that this interval is a distal equivalent of the uppermost Permian coal seams rather than a true correlative of the "marker mudstone" (**Figure 10**). However, the overlying thin transitional interval (between the strongly carbonaceous and greenish siltstones traditionally placed at the base of the Rewan Group) might locally represent the "marker mudstone" (**Figure 10**). No tuffs have been identified in the "marker mudstone" for absolute age dating.

## Macroflora of the Permian-Triassic Transition

Several studies have reported plant macrofossils from shales and siltstones overlying the Vales Point, Bulli and Katoomba seams in various parts of the Sydney Basin. Most have been recovered from coastal exposures and the roof strata of mines in the Bulli district (southern Sydney Basin), coastal outcrops at Frazer Beach (northern Sydney Basin) and cuttings at Coxs Gap railway tunnel (western Sydney Basin; Retallack 1980; Retallack 2002; Vajda et al., 2020). However, in most cases it is unclear whether these fossils derive from the FBM or from fine-grained beds intercalated with the basal sandstones of the overlying Narrabeen Group. Those recorded from the Frazer Beach section (Vajda et al., 2020) derive unequivocally from an interlaminated bed of fine-grained sandstone and siltstone positioned within the lower Dooralong Shale, 1.12–1.44 m above the top of the FBM (= 1.62–1.94 m above the EPE horizon).

Fossil assemblages from the FBM and basal Narrabeen Group characterize a post-extinction flora of modest-diversity (about 16 taxa) representative of the earliest stages of ecosystem recovery. Some of these taxa are defined for specific plant organs (morphotaxa), hence the diversity of reproductively discrete (whole-plant) species represented by plant macrofossils in this unit is substantially lower. A full systematic analysis of this flora is intended for publication elsewhere, but a preliminary list of taxa represented in institutional collections is presented here to illustrate the general composition of the recovery flora, regardless of its precise stratigraphic position (**Table 2**).

The flora contains plant groups ranging from small herbaceous forms to woody shrubs or trees. *Lepidopteris callipteroides* (Peltaspermales) dominates the assemblage, although voltzialean conifer twigs and isolated leaves are also common locally. Most elements of the flora persist higher into the Narrabeen Group and are attributed to the *L. callipteroides* macrofloral zone—roughly of latest Changhsingian to Smithian age (Retallack, 1977; Retallack, 1980; Retallack, 2002). The leaves (or leaf segments) of most plants are diminutive, and those of the gymnosperms typically bear thick cuticles and/or have strong stomatal protection suggestive of adaptation to inhibition of transpirational water loss. Elements of this fossil flora have been described and illustrated by Townrow (1956), Townrow (1960), Townrow (1966), Townrow (1967a), Townrow (1967b), Retallack (1977), Retallack (1980), Retallack (2002), and White

(1981) and interpreted to reflect the establishment of a sclerophyllous vegetation tolerant to seasonal water deficiency (Retallack 2018). A selection of key taxa is illustrated here (**Figure 14**) to highlight the dominant woody and herbaceous components of the paleoflora. Although several plants were sclerophyllous and adapted to seasonal scarcity of moisture, we do not find evidence of xerophytic plants typical of fully arid conditions. The presence of various free-sporing ferns, sphenophytes and lycopsids suggests at least seasonally moist conditions in the aftermath of the EPE in the Sydney Basin.

The presence of *Glossopteris* or its associated ovuliferous (*Plumsteadia*) or root (*Vertebraria*) organs in siltstones above the Bulli Coal and its lateral equivalents is contentious. Various studies (e.g., Dun, 1911; Stuntz, 1965; Townrow, 1966; Helby 1969; McElroy, 1969) have reported the presence of *Glossopteris* above the uppermost Permian coal of the Sydney Basin, but concerted searches by Retallack (1980), Vajda et al. (2020), and Mays et al. (2020) failed to find any reliable evidence of this plant group above the uppermost seam. Perhaps the most convincing evidence is the illustration of a ripple-marked laminated slab hosting numerous *Glossopteris* leaves, possible pleuromeian microphylls and sinuous horizontal invertebrate burrows purported to derive from the roof of the Bulli Coal (Diessel, 1992, figure 6.7). The precise geographic source and stratigraphic position of this slab is unclear and it might represent an intraseam clastic bed high in the Bulli Coal. Much younger records of *Glossopteris* or its associated organs (e.g., from the Middle Triassic to Cretaceous) of Australia (Feistmantel, 1890; Johnston, 1896; Holmes, 1992) appear to be misidentifications of other plant groups (*Gontriglossa* and *Sagenopteris*). A single specimen of *Vertebraria australis* collected by G. Retallack in 1974 and registered in the Australian Museum collections (AMF63722: **Figure 14L**) is stated on the label to derive from the "*callipteroides* Zone" at South Bulli. The precise stratigraphic source of this specimen is uncertain. Similarly, small segmented rootlets reminiscent of *V. australis* were recorded in PHK Bunnerong-1 well immediately above the Bulli Seam (Fielding et al., 2019), but the identification remains tentative. Small leaf fragments from Coxs Gap with anastomosing venation reported by Retallack (1980) might be the remains of *Rochipteris* (Petriellales) foliage rather than *Glossopteris*. Thus far, the evidence for *Glossopteris* persisting into the FBM (above the EPE) is equivocal. If this group did persist above our placement of the EPE, it was only for a brief time and in very low numbers. There is no convincing evidence of glossopterids persisting into the Triassic in Australia or elsewhere.

## Fossil Fauna

Tracks of three large tetrapod animals are known from an interlaminated shale and ripple-marked sandy siltstone around 25–50 cm above the Bulli Coal in roof shales (here equated to the FBM) of Bellambi Colliery (Harper 1915; Retallack, 1996), Kemira Colliery (Clark, 1992), and Oakdale Colliery (Warren, 1997) all in the Southern Sydney Basin. The tracks vary somewhat in size but are probably conspecific. Individual footprints have digits terminated by claws and were assigned to the ichnotaxon *Dicynodontopus bellambiensis* (Retallack, 1996). The Bellambi Colliery footprints are around 60–80 mm long, 40–50 mm wide, with an average stride length of 349 mm (**Figure 15A**), and an external track width of c. 300 mm suggesting a roughly dog-sized, wide-bodied, trackmaker (Retallack, 2005, figure 13). The tracks from Oakdale Colliery are smaller but otherwise similar (**Figure 15D**). Retallack (1996) inferred that the Sydney Basin tracks were most likely produced by the common Gondwanan dicynodont *Lystrosaurus* and Warren (1997) concurred that such traces were probably produced by a dicynodont (therapsid) or procolophonid (parareptile). Burrows of a somewhat smaller vertebrate are known from the type section of the FBM in the northern Sydney Basin (**Figure 15B**). These burrows, assigned to *Reniformichnus australis*, descend from an overbank sandstone into the silty FBM and, in some cases, penetrate the underlying Vales Point coal seam. There is a continuum (normal distribution) of burrow sizes with maximum widths of 40–150 mm and heights of 11–100 mm (McLoughlin et al., 2020). They typically have a bilobate base, and bear weak bioglyphs on their surface (**Figure 15C**). The burrows are similar to forms interpreted as small cynodont burrows described by Sidor et al. (2008) from the Lower Triassic of Antarctica, and by Damiani et al. (2003) and Krummeck and Bordy (2018) from coeval strata in the Karoo Basin, South Africa. The Sydney Basin burrows can not be assigned definitively to any tracemaker in the absence of entombed skeletal remains but are inferred to have been produced by a *Thrinaxodon*-like cynodont—the range of sizes possibly being the result of production by a population of different sexes and age cohorts, together with some post-excavation compression of the burrow forms (McLoughlin et al., 2020). There is no strong evidence in terms of size distribution, shape or excavation traces to segregate these burrows into more than one ichnotaxon.

Invertebrate trackways, similar to *Tasmanadia*, consisting of two parallel rows of obliquely transverse markings were reported by Retallack (1996) on the same bedding plane preserving the tetrapod tracks at Bellambi Colliery, and Warren (1997) also reported invertebrate traces associated with the trackway from Oakdale Colliery. Retallack (1996) suggested that the Bellambi invertebrate trackway could have been produced by various insects. Tillyard (1918) described a fragmentary orthopteran forewing (*Elcanopsis sydneiensis*) from probable correlative shales above the coal seam in the Sydney Harbor Colliery at Balmain. McLoughlin et al. (2020) also reported sparse 1.2-mm-diameter silt-filled invertebrate burrows in a splay sandstone directly overlying the FBM at Frazer Beach, and Diessel (1992), figure 6.7 illustrated sinuous burrows on a bedding plane from laminites above the Bulli Coal in the southern Sydney Basin). Clark (1992) also mentioned the presence of rare burrows of unspecified character in shales overlying the Bulli Coal in the southern Sydney Basin. Bowman (1980) mentioned the occurrence of unionid bivalves in mudrocks above the Bulli Coal but did not illustrate or provide locality details of these specimens. These studies collectively indicate a relatively meagre vertebrate and invertebrate fauna associated with predominantly lacustrine or other floodplain settings during deposition of the


**FIGURE 14 |** Plant macrofossils in historical collections from the shale-dominated interval overlying the Vales Point coal seam and Bulli Coal at various sites within the Sydney Basin (see **Table 2** for taxon authors). In the absence of precise stratigraphic sources, these are inferred to derive primarily from the uppermost part of the Frazer Beach Member or lowermost Dooralong Shale/Coal Cliff Sandstone; all of these strata are assigned to the *Lepidopteris callipteroides* Biozone. **(A)**, *Cyclomeia undulata* (Pleuromeiales), "roof shales" above Bulli Coal, Bellambi Colliery, AMF58791. **(B)**, *Cyclomeia undulata* (Pleuromeiales) "roof shales" above Bulli Coal, Bellambi Colliery, AMF60882. **(C)**, *Cyclomeia undulata* microphyll (Pleuromeiales), "roof shales" above Bulli Coal, South Bulli, AMF63719. **(D)**, Isoetalean or pleuromeian sporophyll, "roof shales" above Bulli Coal, Bellambi Colliery, AMF27421. **(E)**, *Cyclomeia* sp.?, small pleuromeian leafless rhizomorph with attached roots, "roof shales" above Bulli Coal, Bulli, AMF120062. **(F)**, *Schizoneura gondwanensis* (Equisetales), 3.05 m above topmost Permian coal, Birthday Shaft, Balmain, AMF8259. **(G)** *Neocalamites* sp. (equisetalean axis), "roof shales" above Bulli Coal, South Bulli Colliery, AMF91467. **(H)** *Sphenopteris* sp. (Polypodiopsida), "roof shales" above Bulli Coal, Bellambi Colliery, AMF27402. **(I)** *Cladophlebis* sp. (Osmundales), "roof shales" above Bulli Coal, Bellambi Colliery, AMF27406. **(J)** *Rochipteris* sp.? (Petriellales), "roof shales" above Bulli Coal, Bellambi Colliery, AMF27409a. **(K)** *Peltaspermum* sp. (Peltaspermales) or nodal diaphragm (Equisetales), "roof shales" of Bulli Coal, Bellambi Colliery, AMF27425c. **(L)** *Vertebraria australis*, (Glossopteridales root), putatively from the "roof shales" of the Bulli Coal, South Bulli Colliery, AMF63722. **(M)** *Lepidopteris callipteroides* (Peltaspermales), "roof shales" above Bulli Coal, Bulli Colliery, AMF58520. **(N)** Portion of *Lepidopteris callipteroides* pinna (Peltaspermales), sandstone lamina above Bulli Coal, Coal Cliff Beach, AMF51730. **(O)** *Rissikia apiculata* (Voltziales), "roof shales" above Bulli Coal, Bellambi Colliery, AMF27415. **(P)** Isolated bract or seed, "roof shales" of Bulli Coal, South Bulli Colliery, AMF91466. **(Q)** *Voltziopsis africana* (Voltziales), "roof shales" of Bulli Coal, South Bulli Colliery, AMF50149. **(R)** *Rissikia apiculata* (Voltziales), "roof shales" above Bulli Coal, Bellambi Colliery, AMF27423. Scale bars = 10 mm for all figures except P and K (= 1 mm).

**TABLE 2 |** List of the key taxa represented in the Frazer Beach Member or immediately overlying basal beds of the Narrabeen Group based on historical and recent collections held in the Australian Museum, Sydney, and the Swedish Museum of Natural History, Stockholm.

| Plant taxon | Higher taxon | Plant habit | Leaf form | Special adaptations | Relative abundance |
|---|---|---|---|---|---|
| Unidentified lycopsid leaves (**Figure 14D**) | Lycopsida | Herbaceous | Spine-like | | High |
| *Isoetites* sp. (**Figure 14E**) | Isoetales/Pleuromeiales | Herbaceous | Needle-like or scale-like | Basal corm/rhizomorph | Moderate |
| *Cyclomeia undulata* (Burges) White (1981) (**Figures 14A–C**) | Pleuromeiales | Herbaceous to monopodial shrub | Needle-like | Basal corm/rhizomorph | Moderate |
| *Neocalamites* sp. (**Figure 14G**) | Equisetales | Rhizomatous reed-like herbaceous | Spine-like | Rhizomatous, photosynthetic stems? | Low |
| *Schizoneura gondwanensis* Feistmantel (1876) (**Figure 14F**) | Equisetales | Rhizomatous climbing or scrambling herbaceous | Paired broad laminae of fused needle-like leaves | Potential climber on other plants | Moderate |
| *Cladophlebis* sp. A (**Figure 14I**) | Osmundales | Herbaceous | Bipinnate, large | Understorey plant | Low |
| *Cladophlebis* sp. B/*Sphenopteris* sp. (**Figure 14H**) | Osmundales | Herbaceous | Bipinnate, large | Understorey plant | Low |
| *Lepidopteris callipteroides* (Carpentier) Retallack (2002) (**Figures 14N,M**) | Peltaspermales | Woody shrub to tree | Forked, multipinnate, small leaflets | Thick cuticles, papillae-protected stomata. Some preserved as seedlings with cotyledons? | High |
| *Hoegia antevsiana* Townrow (1957) | Peltaspermales | Woody shrub to tree | | | Low |
| *Peltaspermum* sp. (**Figure 14K**) | Peltaspermales | Woody shrub to tree | | Seeds protected on underside of peltate megasporophyll | Low |
| *Rhipidopsis/Rochipteris* sp. (**Figure 14J**) | Ginkgoales or petriellales | Small woody shrub? | Broad, flabellate | | Low |
| *Voltziopsis/Rissikia apiculata* Townrow (1967b) (**Figures 14O,R**) | Voltziales | Small woody tree? | Small, awl-shaped | Leaf bases locally appressed to axis. Thick cuticle | Moderate |
| *Voltziopsis africana* Seward (1934) (**Figure 14Q**) | Voltziales | Small woody tree? | Small, elliptical | Thick cuticle | Moderate |
| *Vertebraria australis* (?) McCoy (1847) (**Figure 14L**) | Glossopteridales (Dictyopteridiales) | Roots of woody tree | N/A | Segmented into air chambers for growth in waterlogged soils | Low |
| Dispersed seed or bract (**Figure 14P**) | Incertae sedis | ? | N/A | | Low |

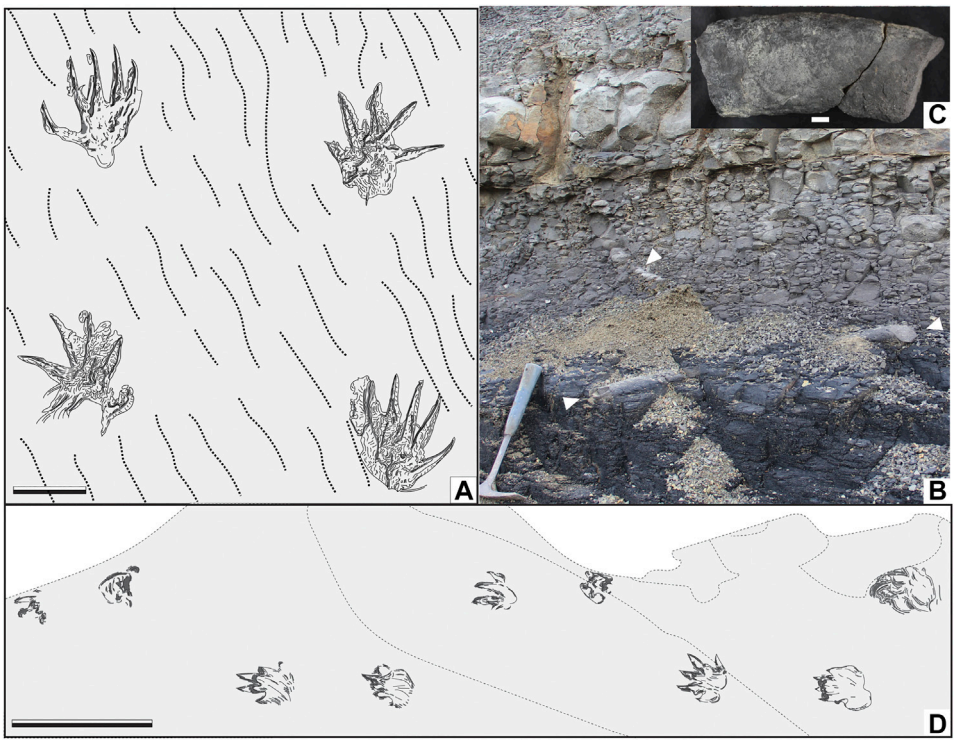


**FIGURE 15 |** Vertebrate trace fossils from the Frazer Beach Member. **(A)** Line-drawing of probable lystrosaurid trackway from the "roof shales" above the Bulli Coal, Bellambi Colliery (trackway originally illustrated by Harper (1915), pl. 24, and Retallack (1996, figure 3). Dotted lines indicate the crests of symmetrical ripples on the bedding plane. **(B)** Probable cynodont burrows filled with sandstone (arrowed) transecting the Frazer Beach Member in the type section. The burrow entrances appear to be positioned at the level of the basal massive splay sandstone bed of the overlying Dooralong Shale. **(C)** Surface texture of a sand-filled burrow showing weakly defined bioglyphs (excavation marks). **(D)** Line-drawing of a dicynodont or procolophonid trackway from the "roof shales" of Oakdale Colliery (original illustrated by Warren (1997, figure 8). Dotted lines indicate fractures in the rock. Scale bars = 50 mm for **(A, D)**, 10 mm for **(C)**; hammer in **(B)** = 28 cm.

FBM. In addition, Mishra et al. (2019) recorded spinose thecamoebid (Amoebozoa) testae from an unspecified position within a section through the uppermost Moon Island Beach Formation at Wybung Head. It is possible that these represent part of the impoverished post-EPE biota of the FBM, but it is more likely that they derive from the underlying Vales Point coal seam.

## Regional Depositional Framework and Paleoclimate

The overall depositional environment both before and after accumulation of the FBM in the Sydney Basin was a lowland, probably coastal, alluvial plain crossed by sand- and gravel-bed rivers of varying size and planform. Predominantly southward-directed river systems drained the Bowen-Gunnedah-Sydney basin complex at this time, with significant contributions of sediment derived from the rising New England Orogen to the east, and lesser additions from the stable craton to the west (Ward 1972; Fielding et al., 2001; Fielding et al., 2020). Facies distributions suggest minimal long-term changes in fluvial style, and paleocurrent data indicate little change in the overall dispersal pattern across the EPE in the Sydney Basin (Fielding et al., 2020). The FBM, therefore, represents a temporary disruption of the lowland landscape in response to an ecological perturbation (probably induced by a temperature- and/or moisture-related tipping point) that eliminated deciduous hygrophilous glossopterid forests during the terrestrial EPE. Extensive but ephemeral ponding in the landscape appears to have resulted from the termination of organic accumulation following extinction of the glossopterid-dominated mire forests and the submergence of the abandoned peat surface owing to rising water tables, continued subsidence, compaction, and microbial oxidation of the peat profile, together with temporary retention of coarse clastic sediments in proximal portions of the drainage system.

The latest Permian, glossopterid-dominated, peat-forming vegetation of the Sydney Basin has been interpreted to characterize consistently moist climates under a pronounced photoperiod regime (Holmes, 1995; McLoughlin et al., 2019). Glossopterids were broad-leafed, deciduous, tall trees with aerated root systems especially adapted to growth in waterlogged substrates (McLoughlin, 2011). In contrast, the flora of the post-EPE *Lepidopteris callipteroides* macrofloral zone (?upper FBM to lower Narrabeen Group) is characterized by gymnosperms with small (generally <2 cm long) leaves or leaf segments, thick cuticles, and strongly protected stomata—all features of sclerophyllous plants typically adapted to warmth

and seasonal water shortages. The post-EPE flora also contains an array of opportunistic herbaceous plants (**Table 2**) with free-sporing life cycles likely tied to episodic water availability. On this basis, we infer at least seasonally intensified moisture deficiency, but not fully arid conditions, affecting the vegetation in the immediate aftermath of the EPE. Post-EPE ponded settings were not sufficiently persistent, or the surviving peltasperm-conifer vegetation was not adequately adapted to the development of complex mire communities, to enable peat accumulation. Paleoclimate simulations adjusted for amplified levels of atmospheric $CO_2$ derived from outgassing associated with Siberian Trap volcanism, coupled with CIA signatures of the sedimentary rocks, indicate increasingly seasonal conditions through the last 0.7–1.3 myrs of the Permian (Fielding et al., 2019; T. Frank, unpublished data). This culminated in a short phase of intense chemical weathering and environmental instability during the EPE and accumulation of the FBM. Up-section increases in the representation of desiccation features, ferruginous concretions, and microspherulitic siderite in paleosols also attest to a long-term drying trend in the Early Triassic, although log impressions up to 20 cm wide in the basal Narrabeen Group indicate conditions remained favorable for forest growth (Retallack, 1999). Paleosol chemistry has been employed to infer mean annual precipitation of 1,000–1,300 mm during deposition of both the latest Permian coal-bearing succession and the FBM, and a reduction to 800–1,200 mm per annum during deposition of the Dooralong Shale (c. 1–11 m above the topmost coal: Retallack, 1999). Collectively, the paleontological, geochemical, and modeling evidence suggests a long-term warming and (at least seasonal) drying trend through the Permian-Triassic transition, punctuated by a pulse of enhanced chemical weathering during deposition of the FBM.

## DISCUSSION AND CONCLUSIONS

The newly defined Frazer Beach Member represents a distinctive, laterally extensive sheet of predominantly lacustrine shales and siltstones that accumulated in the wake of the EPE in the Sydney Basin. It represents a useful marker for lithostratigraphic correlation and accumulated over a few thousand years (Vajda et al., 2020) at the end of the Permian. Equivalent facies are recognizable in adjoining basins to the north, within the informally designated "marker mudstone." Similar facies are also represented in equivalent stratigraphic positions across Gondwana, e.g., in Antarctica, Africa, and India.

The FBM and its lateral correlatives are characterized by depauperate vertebrate and invertebrate ichnofossil and spore-pollen-algae suites and enrichment in charcoal and fungi typical of a post-extinction "dead zone." This combination of simple sedimentary features and impoverished fossil biota dominated by fungi and bacterially generated amorphous organic matter is the terrestrial equivalent of anachronistic facies that are commonly recognized in marine strata in the aftermath of major extinction events (Maaleki-Moghadam et al., 2019). Proliferation of fungal/algal remains (some of probable terrestrial origin) and amorphous organic matter is also a feature typical of post-EPE shallow marine palynoassemblages globally (Haig et al., 2015; Spina et al., 2015; Rampino and Eshet, 2018). Accumulation of the FBM occurred after the extinction of glossopterid-dominated arborescent peatland communities. At that time, significant organic accumulation ceased but ongoing compaction of the previously deposited peat and continuing subsidence of the depositional surface provided accommodation space for the development of extensive shallow lacustrine systems on alluvial plains. The cause of glossopterid extinction at the EPE remains unclear but is likely to be related to an environmental tipping point (e.g., excessive heat or seasonal drought) similar to those factors that primarily control the distribution of the dominant plants in modern boreal forests (Churkina and Running, 1998; Gilliam, 2016). The long-term warming and drying trends inferred for the Permian-Triassic transition are punctuated by a brief interval of enhanced chemical weathering during deposition of the FBM. The conditions favoring accumulation of the predominantly fine-grained FBM were short-lived and more typical fluvial systems of the Narrabeen Group and equivalent strata were re-established a few thousand years after the EPE. A sparse and low-diversity recovery flora, dominated by woody sclerophyllous Peltaspermales and Voltziales, and herbaceous Isoetales/Pleuromeiales, sphenophytes and ferns became established around the end of FBM accumulation, but peat-forming ecosystems producing economic quantities of coal did not recover in the region for at least 10 million years (Retallack et al., 1996; Vajda et al., 2020).

Ash beds dated by CA-IDTIMS analyses of zircon crystals now provide the Sydney Basin succession with the best age and stratigraphic constraints on the EPE and PTB in Gondwana. The terrestrial expression of the EPE in the Sydney Basin is dated to c. 252.3–252.1 Ma or roughly 200–400 kyrs before the PTB and c. 160–360 kyrs before the onset of the tropical marine extinction (with the provision that these are maximum depositional ages). This offset in terrestrial vs. marine extinctions is consistent with recent records from South Africa and China (Chu et al., 2020; Gastaldo et al., 2020). The cause(s) behind such a long lag time between the terrestrial and marine extinctions remain uncertain, but may relate to the much earlier response of hygrophilous temperate-zone plant communities to drought or abrupt warming compared to equatorial warm-water oceanic communities that were buffered from such changes. We note that additional high-precision dating of beds within the Vales Point coal seam, FBM, and basal Narrabeen Group might narrow the perceived temporal gap between these events. The pattern of terrestrial extinction and recovery at the EPE has similarities to the end-Cretaceous event in terms of sharp extinction or decline of some major woody plant groups (Vajda and Bercovici, 2014; McLoughlin, 2020), loss of large vertebrates (Huttenlocker, 2014; Botha et al., 2020; Khosla and Lucas, 2020; Smith et al., 2020) and initial re-establishment of pteridophyte-rich plant communities (Vajda and McLoughlin, 2007; Feng et al., 2020). However, the recovery of the biota after the EPE was greatly protracted in comparison to the early Paleocene. The combination of numerous CA-IDTIMS dates and a well-resolved palynostratigraphic zonation makes the Sydney Basin succession the primary reference for the correlation of terrestrial upper Permian–Lower Triassic strata in the Southern Hemisphere and provides the principal framework for understanding the evolution of

the southern high-paleolatitude terrestrial biota through Earth's largest extinction event.

## DATA AVAILABILITY STATEMENT

The datasets presented in this study can be found in online repositories. The names of the repository/repositories and accession number(s) can be found in the article/ Supplementary Material.

## AUTHOR CONTRIBUTIONS

SM contributed the paleobotany, geophysics, geotechnical discussion and coordinated the study. RN and JC contributed the CA-IDTIMS data and the discussion on geochronological controls on the stratigraphy. VV and CM contributed the palynology of the Sydney Basin succession. CF contributed the sedimentological and petrographic data. TF contributed the geochemical and isotopic data. AW contributed the palynology of the Bowen and Galilee Basin successions. MB contributed borehole data and information on the regional distribution of strata. All authors contributed to the development of the manuscript, the Discussion of the results, and the writing of the text.

## FUNDING

Funding from Vetenskapsrådet and the National Science Foundation collectively supported fieldwork in Australia, laboratory analysis of samples and manuscript preparation costs.

## ACKNOWLEDGMENTS

The authors acknowledge the support of the Swedish Research Council (VR) grants 2018-04527 to SM, and 2015-4264 and 2019-04061 to VV, and a collaborative research grant from the National Science Foundation (EAR-1636625 to CF and TF). We thank two reviewers for their constructive comments on the manuscript.

## REFERENCES

Agnew, D., Bocking, M., Brown, K., Ives, M., Johnson, D., Howes, M., et al. (1995). "Sydney basin—Newcastle Coalfield," in *Geology of Australian coal basins*. Editors C. R. Ward, H. J. Harrington, C.W. Mallett, and J. W. Beeston (Sydney: Geological Society of Australia, Coal Geology Group, Special Publication 1), 197–212.

Armstrong, M., Bamberry, W. J., Hutton, A. C., and Jones, B. G. (1995). "Southern coalfield," in *Geology of Australian coal basins*. Editors C. R. Ward, H. J. Harrington, C. W. Mallett, and J. W. Beeston (Sydney: Geological Society of Australia, Coal Geology Group, Special Publication 1), 213–230.

Balme, B. E. (1969). The Permian-Triassic boundary in Australia. *Geol. Soc. Aus. Spec. Publ.* 2, 99–112.

Balme, B. E. and Hennelly, J. P. F. (1956). Monolete, monocolpate, and alete sporomorphs from Australian Permian sediments. *Aust. J. Bot.* 4, 54–67.

Batten, D. J. (1996). "Chapter 26A. Palynofacies and palaeonvironmental interpretation," in *Palynology: principles and applications*. Editors J. Jansonius and D.C. McGregor (Los Angeles: American Association of Stratigraphic Palynologists Foundation), 1011–1064.

Becker, L., Poreda, R. J., Basu, A. R., Pope, K. O., Harrison, T. M., Nicholson, C., et al. (2004). Bedout: a possible end-Permian impact crater offshore of northwestern Australia. *Science* 304, 1469–1476. doi:10.1126/SCIENCE.1093925

Bembrick, C. S. (1980). "Geology of the Blue Mountains, western Sydney Basin," in *A guide to the Sydney Basin*. Editors C. Herbert and R. Helby (Sydney: New South Wales Geological Survey Bulletin), Vol. 26, 134–161.

Bembrick, C. S. (1983). Stratigraphy and sedimentation of the late Permian Illawarra coal measures in the Western Coalfield, Sydney Basin, New South Wales. *J. Proc. Roy. Soc. NSW* 116, 105–117.

Bharadwaj, D. C. and Salujha, S. K. (1964). Sporological study of seam VIII in Raniganj Coalfield, Bihar (India)–Part I. Description of sporae dispersae. *Palaeobotanist* 12, 181–215.

Booker, F. W. (1960). Studies in Permian sedimentation in the Sydney Basin, New South Wales. *Geol. Surv. NSW, Dept. Mines Rep.* 5, 10–62.

Botha, J., Huttenlocker, A. K., Smith, R. M. H., Prevec, R., Viglietti, P., and Modesto, S. (2020). New geochemical and palaeontological data from the Permo-Triassic boundary in the South African Karoo Basin test the synchrony of terrestrial and marine extinctions. *Palaeogeogr. Palaeoclimatol. Palaeoecol.* 540, 109469. doi:10.1016/j.palaeo.2019.109467

Bowman, H. N. (1980). "Southern Coalfield, upper Shoalhaven Group and Illawarra coal measures," in *A guide to the Sydney Basin*. Editors C. Herbert and R. Helby (Sydney: New South Wales Geological Survey Bulletin), Vol. 26, 116–132.

Branagan, D. F. (1972). *Geology and coal mining in the Hunter Valley 1791–1861, Newcastle history monographs 6*. Newcastle: Newcastle Public Library.

Bryan, J. H., McElroy, C. T., and Rose, G. (1966). *Sydney 1:250,000 geological series explanatory notes*. 3rd Edn. Sydney: Geological Survey of New South Wales.

Burgess, S. D., Bowring, S., and Shen, S.-z. (2014). High-precision timeline for Earth's most severe extinction. *Proc. Nat. Acad. Sci. U.S.A.* 111, 3316–3321. doi:10.1073/pnas.1317692111

Chu, D., Grasby, S. E., Song, H., Corso, J. D., Wang, Y., Mather, T. A., et al. (2020). Ecological disturbance in tropical peatlands prior to marine Permian-Triassic mass extinction. *Geology* 48, 288–292. doi:10.1130/G46631.1

Churkina, G. and Running, S. W. (1998). Contrasting climatic controls on the estimated productivity of global terrestrial biomes. *Ecosystems* 1, 206–215. doi:10.1007/s100219900016

Clare, R. C. (1985). "Geology of the Newlands mine area," in Proceedings of the Bowen Basin Coal Symposium (Rockhampton: Geological Society of Australia), 284–292.

Clark, B. R. (1992). Depositional environment of the Bulli Coal in the Southern Coalfield of New South Wales and its effect on quality characteristics. MSc thesis. Wollongong: The University of Wollongong, 161, (unpublished).

Collinson, J. W., Hammer, W. R., Askin, R. A., and Elliot, D. H. (2006). Permian-Triassic boundary in the central transantarctic Mountains, Antarctica. *Geol. Soc. Amer. Bull.* 118, 747–763. doi:10.1130/B25739.1

Creech, M. (2002). Tuffaceous deposition in the Newcastle Coal Measures: challenging existing concepts of peat formation in the Sydney Basin, New South Wales, Australia. *Int. J. Coal Geol.* 51, 185–214. doi:10.1016/S0166-5162(02)00084-8

Damiani, R., Modesto, S., Yates, A., and Neveling, J. (2003). Earliest evidence of cynodont burrowing. *Proc. R. Soc. Lond. B* 270, 1747–1751. doi:10.1098/rspb.2003.2427

David, T. W. E. (1907). The geology of the Hunter River coal measures. *Geol. Surv. NSW Mem.* 4, 1–372.

David, T. W. E. (1950). *The geology of the Commonwealth of Australia 1*. London: Edward Arnold.

de Jersey, N. J. (1962). Triassic spores and pollen grains from the Ipswich Coalfield. *Geol. Surv. Qld. Pub.* 307, 1–18.

de Jersey, N. J. (1979). Palynology of the Permian-Triassic transition in the western Bowen Basin. *Geol. Surv. Qld. Pub.* 374, 1–39.

de Jersey, N. J. and Hamilton, M. (1967). Triassic spores and pollen grains from the Moolayember Formation. *Geol. Surv. Qld. Publ.* 336, 1–61.

de Jersey, N. J. and Raine, J. I. (1990). Triassic and earliest Jurassic miospores from the Murihiku Supergroup, New Zealand. *New Zeal. Geol. Surv. Paleontol. Bull.* 62, 1–164.

Diessel, C. F. K. (1992). *Coal-bearing depositional systems*. Berlin: Springer.

Diessel, C. F. K., Driver, R. C., and Moelle, K. H. R. (1967). Some geological investigations into a fossil river system in the roof strata of the Bulli Seam, Southern Coalfield. *AUSIMM Proc.* 221, 19–37.

Diessel, C. F. K. and Moelle, K. H. R. (1965). "The application of analysis of the sedimentary and structural features of a coal seam and its surrounding strata to the operations of mining," in *Eighth Commonwealth Mining and Metallurgy Congress, Australia and New Zealand, 22nd technical session, coal mining*. Editors J. T. Woodcock, R. T. Madigan, and R. G. Thomas (Melbourne: Australasian Institute of Mining and Metallurgy), 837–856.

Draper, J. J. (2002). *Geology of the Cooper and Eromanga basins, Queensland*. Queensland minerals and energy review series. Brisbane: Queensland Department of Natural Resources and Mines.

Dun, W. S. (1910). Notes on some fossil plants from the roof of the coal seam in the Sydney Harbour Colliery. *J. Proc. Roy. Soc. NSW* 44, 615–619.

Dun, W. S. (1911). Additions to the Permo-Carboniferous flora of New South Wales, No. 2. *Rec. Geol. Surv. NSW* 6, 46–51.

Evans, P. R. (1966). Mesozoic stratigraphic palynology in Australia. *Australas. Oil Gas J.* 12, 58–63.

Fairbridge, R. W. (1953). *Australian stratigraphy*. 2nd Edn. Perth: University of Western Australia Textbooks Board.

Feistmantel, O. (1876). Notes on the age of some fossil floras of India. *Rec. Geol. Surv. India* 9, 63–79.

Feistmantel, O. (1890). Geological and palaeontological relations of the coal and plant-bearing beds of Palaeozoic and Mesozoic age in eastern Australia and Tasmania, with special reference to the fossil flora. *Mem. Geol. Surv. NSW, Palaeont.* 3, 1–183.

Feng, Z., Wie, H.-B., Guo, Y., He, X.-Y., Sui, Q., Zhou, Y., et al. (2020). From rainforest to herbland: new insights into land plant responses to the end-Permian mass extinction. *Earth Sci. Rev.* 204, 103153. doi:10.1016/j.earscirev.2020.103153

Fielding, C. R., Frank, T. D., Tevyaw, A. P., Savatic, K., Vajda, V., McLoughlin, S., et al. (in press 2020). Sedimentology of the continental end-Permian extinction event in the Sydney Basin, eastern Australia. *Sedimentology* doi:10.1111/sed.12782

Fielding, C. R., Frank, T. D., Vajda, V., McLoughlin, S., Mays, C., Tevyaw, A. P., et al. (2019). Age and pattern of the southern high-latitude continental end-Permian extinction constrained by multiproxy analysis. *Nat. Comm.* 10, 385. doi:10.1038/s41467-018-07934-z

Fielding, C. R., Sliwa, R., Holcombe, R. J., and Jones, A. T. (2001). "A new palaeogeographic synthesis for the Bowen, Gunnedah and Sydney Basins of eastern Australia," in *Eastern Australasian Basins Symposium. Petroleum Exploration Society of Australia special publication*. Editors K.C. Hill and T. Bernecker (Melbourne: Australasian Institute of Mining and Metallurgy), 269–278.

Foster, C. B. (1979). Permian plant microfossils of the Blair Athol Coal Measures, Baralaba Coal Measures, and basal Rewan Formation of Queensland. *Geol. Surv. Qld. Publ.* 372, 1–244.

Foster, C. B. (1982). Spore-pollen assemblages of the Bowen Basin, Queensland (Australia): their relationship to the Permian/Triassic boundary. *Rev. Palaeobot. Palynol.* 36, 165–183.

Gastaldo, R. A., Adendorff, R., Bamford, M., Labandeira, C. C., Neveling, J., and Sims, H. (2005). Taphonomic trends of macrofloral assemblages across the Permian–Triassic boundary, Karoo Basin, South Africa. *Palaios* 20, 479–497.

Gastaldo, R. A., Kamo, S. L., Neveling, J., Geissman, J. W., Bamford, M., and Looy, C. V. (2015). Is the vertebrate-defined Permian-Triassic boundary in the Karoo Basin, South Africa, the terrestrial expression of the end-Permian marine event?. *Geology* 43, 939–942.

Gastaldo, R. A., Kamo, S. L., Neveling, J., Geissman, J. W., Looy, C. V., and Martini, A. M. (2020). The base of the *Lystrosaurus* Assemblage Zone, Karoo Basin, predates the end-Permian marine extinction. *Nat. Comm.* 11, 1428. doi:10.1038/s41467-020-15243-7

Gastaldo, R. A., Neveling, J., Geissman, J. W., and Kamo, S. L. (2018). A lithostratigraphic and magnetostratigraphic framework in a geochronologic context for a purported Permian–Triassic boundary section at Old (West) Lootsberg Pass, Karoo Basin, South Africa. *Geol. Soc. Am. Bull.* 130, 1411–1438.

Gastaldo, R. A. and Rolerson, M. W. (2008). *Katbergia* gen. nov., a new trace fossil from upper Permian and Lower Triassic rocks of the Karoo Basin: implications for palaeoenvironmental conditions at the P/Tr extinction event. *Palaeontology* 51, 215–229.

Gilliam, F. S. (2016). Forest ecosystems of temperate climatic regions: from ancient use to climate change. *New Phytol.* 212, 871–887. doi:10.1111/nph.14255

Gray, A. R. G. (2000). Amendments to the stratigraphy of the Early Triassic Arrabury Formation in the Cooper Basin. *Qld. Govt. Min. J.* 101, 32–38.

Grebe, H. (1970). Permian plant microfossils from the Newcastle Coal Measures/Narrabeen Group boundary, Lake Munmorah, New South Wales. *Rec. Geol. Surv. NSW* 12, 125–136.

Haig, D., Martin, S. K., Mory, A. J., McLoughlin, S., Backhouse, J., Berrell, R. W., et al. (2015). Early Triassic (early Olenekian) life in the interior of East Gondwana: mixed marine-terrestrial biota from the Kockatea Shale, Western Australia. *Palaeogeog., Palaeoclimatol., Palaeoecol.* 471, 511–533. doi:10.1016/j.palaeo.2014.10.015

Hankel, O. (1992). Late Permian to Early Triassic microfloral assemblages from the Mayiya Chumvi Formation, Kenya. *Rev. Palaeobot. Palynol.* 72, 129–147.

Hansen, H. J., Lojen, S., Toft, P., Dolenec, T., Jinan, T., Michaelsen, P., et al. (2000). "Magnetic susceptibility and organic carbon isotopes of sediments across some marine and terrestrial Permo-Triassic boundaries," in *Permian-Triassic evolution of Tethys and western circum-Pacific*. Editors H. Yin, J. M. Dickins, G. R. Shi, and J. Tong (Amsterdam: Elsevier), 271–289.

Harper, L. E. (1915). Geology and mineral resources of the Southern Coal-field. *Geol. Mem. Geol. Surv. NSW* 7, 1–410.

Harrington, H. J., Brakel, A. T., Hunt, J. W., Wells, A. T., Middleton, M. F., O'Brien, P. E., et al. (1989). Permian coals of eastern Australia. *Bur. Min. Res. Bull.* 231, 1–412.

Harvey, C. R. and Singh, R. N. (1998). "A review of fatal outburst incidents in the Bulli Seam," in *In coal 1998: coal operators' conference*. Editor N. Aziz (Wollongong: University of Wollongong and the Australasian Institute of Mining and Metallurgy), 649–658.

Helby, R. J, (1969). "The age of the Narrabeen Group as implied by the microfloras," in *The geology of new south wales*. The Sydney Basin, V. (Sydney: Geological Society of Australia), 404–405.

Helby, R. J. (1970). A biostratigraphy of the late Permian and Triassic of the Sydney Basin. PhD thesis. Sydney: University of Sydney, 513. (unpublished).

Helby, R. J. (1973). Review of late Permian and Triassic palynology of New South Wales. *Geol. Soc. Aus. Spec. Pub.* 4, 141–155.

Helby, R. J., Morgan, R., and Partridge, A. D. (1987). A palynological zonation of the Australian Mesozoic. *Mem. Assoc. Aust. Palaeontol.* 4, 1–94.

Hennelly, J. P. F. (1958). Spores and pollens from a Permian-Triassic transition. *N.S.W. Proc. Linn. Soc. NSW* 83, 363–369.

Herbert, C. (1997). Sequence stratigraphic analysis of Early and Middle Triassic alluvial and estuarine facies in the Sydney Basin, Australia. *Aust. J. Earth Sci.* 44, 125–143. doi:10.1080/08120099708728299

Holmes, W. B. K. (1992). "*Glossopteris*-like leaves in the Triassic of eastern Australia," in *Proceedings of the Birbal Sahni centenary palaeobotanical conference*. Editors B. S. Venkatachala, K. P. Jain, and N. Awasthi (Lucknow: The Birbal Sahni Institute of Palaeobotany), 119–125.

Holmes, W. B. K. (1995). "The late Permian megafossil flora from Cooyal, New South Wales, Australia," in *Global environment and diversification of plants through geological time, Birbal Sahni centenary volume*. Editor D. D. Pant (Allahabad: South Asian Publishers), 123–152.

Huttenlocker, A. K. (2014). Body size reductions in nonmammalian eutheriodont therapsids (Synapsida) during the end-Permian mass extinction. *PloS One* 9 (2), e87553. doi:10.1371/journal.pone.0087553

Hutton, A. and Bamberry, J. (1999). Stratigraphy and terminology for the Southern Coalfield. *Coalfield Geol. Counc. NSW Bull.* 1, 120–152.

Illawarra Coal, (2020). Old Bulli Colliery. https://www.illawarracoal.com/minebase/minebase-a-c/276-old-bulli-colliery.html (Accessed July 3, 2020).

Ives, M., Brinton, J., Edwards, J., Rigby, R., Tobin, C., and Weber, C. R. (1999). Revision of the stratigraphy of the Newcastle Coal Measures. *Coalfield Geol. Counc. NSW Bull.* 1, 113–119.

Jain, R. K. (1968). Middle triassic pollen grains and spores from Minas de Petroleo beds of the Cacheuta Formation (Upper Gondwana), Argentina. *Palaeontog. Abt. B* 122, 1–47.

Johnston, R. M. (1896). Further contributions to the history of the fossil flora of Tasmania. Parts 1 and 2. *Pap. Proc. Roy. Soc. Tas.* 1894–1895, 57–63.

Jorgensen, P. J. and Fielding, C. R. (1996). Facies architecture of alluvial floodbasin deposits: three-dimensional data from the Upper Triassic Callide Coal Measures of east-central Queensland, Australia. *Sedimentology* 43, 479–495. doi:10.1046/j.1365-3091.1996.d01-25.x

Khosla, A. and Lucas, S. G. (2020). "End-Cretaceous extinctions," in *Encyclopedia of geology*. Editors S. Elias and D. Alderton 2nd Edn. (Amsterdam: Elsevier). doi:10.1016/B978-0-12-409548-9.12473-X

Klootwijk, C. (2016). Paleomagnetism of the Carboniferous Rouchel Block, Tamworth Belt, and pole path revision for the new England Orogen, eastern Australia. *Aust. J. Earth Sci.* 63, 513–549. doi:10.1080/08120099.2016.1223170

Krummeck, W. D. and Bordy, E. M. (2018). *Reniformichnus katikatii* (new ichnogenus and ichnospecies): continental vertebrate burrows from the Lower Triassic, main Karoo Basin. *S. Afr.: Ichnos* 25, 138–149. doi:10.1080/10420940.2017.1292909

Laurie, J. R., Bodorkos, S., Nicoll, R. S., Crowley, J. L., Mantle, D. J., Mory, A. J., et al. (2016). Calibrating the middle and late Permian palynostratigraphy of Australia to the geologic time-scale via U–Pb zircon CA-IDTIMS dating. *Aust. J. Earth Sci.* 63, 701–730. doi:10.1080/08120099.2016.1233456

Lindström, S. and McLoughlin, S. (2007). Synchronous palynofloristic extinction and recovery after the end-Permian event in the Prince Charles Mountains, Antarctica: implications for palynofloristic turnover across Gondwana. *Rev. Palaeobot. Palynol.* 145, 89–122. doi:10.1016/j.revpalbo.2006.09.002

Looy, C. V., Twitchett, R. J., Dilcher, D. L., van Konijnenburg-van Cittert, J. H. A., and Visscher, H. (2001). Life in the end-Permian dead zone. *Proc. Nat. Acad. Sci. U.S.A.* 98, 7879–7883. doi:10.1073/pnas.131218098

Maaleki-Moghadam, M., Rafiei, B., Richoz, S., Woods, A. D., and Krystyn, L. (2019). Anachronistic facies and carbon isotopes during the end-Permian biocrisis: evidence from the mid-Tethys (Kisejin, Iran). *Palaeogeog. Palaeoclimatol. Palaeoecol.* 516, 364–383. doi:10.1016/j.palaeo.2018.12.007

Mantle, D. J., Kelman, A. P., Nicoll, R. S., and Laurie, J. R. (2010). *Australian biozonation chart 2010. Part 1: Australian and selected international biozonation schemes tied to the GTS 2004 geological timescale*. Canberra: Geoscience Australia.

Matheson, S. G. (1990). Coal geology and exploration in the Rangal Coal Measures, north Bowen Basin. *Qld. Geol.* 1, 74.

Mays, C., Vajda, V., Frank, T. D., Fielding, C. R., Nicoll, R. S., Tevyaw, A. P., et al. (2020). Refined Permian–Triassic floristic timeline reveals early collapse and delayed recovery of south polar terrestrial ecosystems. *Geol. Soc. Am. Bull.* 132, 1489–1513. doi:10.1130/B35355.1

Mays, C., Vajda, V., and McLoughlin, S. (2021). Permian–Triassic non-marine algae of Gondwana—distributions, natural affinities, ecological implications and extinction patterns. *Earth-Sci. Rev.* 212, 103382. doi:10.1016/j.earscirev.2020.103382

McCoy, F. (1847). On the fossil botany and zoology of the rocks associated with the coal in Australia. *Ann. Mag. Nat. Hist.* 20, 145–157.

McElroy, C. T. (1969). "Triassic system: Narrabeen group," in *The geology of New South Wales*. V. The Sydney Basin. Editor G. H. Packham (Sydney: Geological Society of Australia), 388–407.

McKenzie, P. J. and Britten, R. A. (1969). "Permian of the Hunter Valley–Newcastle Coal Measures," in *The geology of New South Wales*. V. The Sydney Basin Editor G. H. Packham (Sydney: Geological Society of Australia), 339–350.

McLennan, S. M. (1993). Weathering and global denudation. *J. Geol.* 101, 295–303.

McLoughlin, S. (2011). *Glossopteris*: insights into the architecture and relationships of an iconic Permian Gondwanan plant. *J. Bot. Soc. Bengal* 65, 1–14.

McLoughlin, S. (2020). "History of life: plants: gymnosperms". in *Encyclopedia of geology*. 2nd Edn, Editors S. Elias and D. Alderton (Amsterdam: Elsevier), 25. doi:10.1016/B978-0-08-102908-4.00068-0

McLoughlin, S., Lindström, S., and Drinnan, A. N. (1997). Gondwanan floristic and sedimentological trends during the Permian-Triassic transition: new evidence from the Amery group, northern Prince Charles Mountains, East Antarctica. *Antarct. Sci.* 9, 281–298.

McLoughlin, S., Maksimenko, A., and Mays, C. (2019). A new high-paleolatitude late Permian permineralized peat flora from the Sydney Basin, Australia. *Int. J. Plant Sci.* 180, 513–539. doi:10.1086/702939

McLoughlin, S., Mays, C., Vajda, V., Bocking, M., Frank, T. D., and Fielding, C. R. (2020). Dwelling in the dead zone—vertebrate burrows immediately succeeding the end-Permian extinction event in Australia. *Palaios* 35, 342–357. doi:10.2110/palo.2020.007

McMinn, A. (1993). "Palynostratigraphy," in *The Gunnedah Basin, New South Wales*. Editor N. Z. Tadros (Sydney: Geological Survey of New South Wales, Memoir Geology), Vol. 12, 135–143.

Metcalfe, I., Crowley, J. L., Nicoll, R. S., and Schmitz, M. (2015). High-precision U-Pb CA-TIMS calibration of Middle Permian to Lower Triassic sequences, mass extinction and extreme climate-change in eastern Australian Gondwana. *Gondwana Res.* 28, 61–81. doi:10.1016/j.gr.2014.09.002

Michaelsen, P. (1999). Development of late Permian coal Measures, northern Bowen basin, Australia. PhD thesis. Townsville (QLD): James Cook University, 410 (unpublished).

Michaelsen, P. (2002). Mass extinction of peat-forming plants and the effect on fluvial styles across the Permo-Triassic boundary, Bowen Basin, Australia. *Palaeogeog., Palaeoclimatol., Palaeoecol.* 179, 173–188. doi:10.1016/S0031-0182(01)00413-8

Michaelsen, P., Foster, C. B., and Henderson, R. A. (1999). "Destabilisation and collapse of a long-lived (c. 9 My) peat mire ecosystem and dramatic changes of alluvial architecture: Permian–Triassic boundary, northern Bowen Basin, Australia," in *International Conference on Pangea and the Paleozoic–Mesozoic Transition, Wuhan, China, 9–11 march, 1999*. Editors H. Yin and J. Tong (Wuhan: University of Geosciences Press), 137–140.

Michaelsen, P., Henderson, R. A., Crosdale, P. J., and Mikkelsen, S. O. (2000). Facies architecture and depositional dynamics of the upper Permian Rangal Coal Measures, Bowen Basin, Australia. *J. Sediment. Res.* 70, 879–895. doi:10.1306/2DC4093F-0E47-11D7-8643000102C1865D

Mishra, S., Jha, N., Stebbins, A., Brookfield, M., and Hannigan, R. (2019). Palaeoenvironments, flora, and organic carbon and nitrogen isotope changes across the non-marine Permian-Triassic boundary at Wybung Head, Australia. *Palaeogeog. Palaeoclimatol. Palaeoecol.* 534, 109292. doi:10.1016/j.palaeo.2019.109292a

Moczydłowska, M. and Willman, S. (2009). Ultrastructure of cell walls in ancient microfossils as a proxy to their biological affinities. *Precambrian Res.* 173, 27–38. doi:10.1016/j.precamres.2009.02.006

Moffitt, R. S. (1982). The 1980 east Muswellbrook coal drilling programme. *Geol. Surv. NSW Quart. Notes* 47, 17–26.

Nesbitt, H. W. and Young, G. M. (1982). Early Proterozoic climates and plate motions inferred from major element chemistry of lutites. *Nature* 299, 715–717.

Neveling, J., Gastaldo, R. A., and Geissman, J. W. (2016). The Permo–Triassic boundary in the Karoo Basin. *Field Trip Guide PRE* 3, 22–27 Cape Town: 35th International Geological Congress.

Pacton, M., Gorin, G. E., and Vasconcelos, C. (2011). Amorphous organic matter—experimental data on formation and the role of microbes. *Rev. Palaeobot. Palynol.* 166, 253–267. doi:10.1016/j.revpalbo.2011.05.011

Phillips, L. J., Crowley, J. L., Mantle, D. J., Esterle, J. S., Nicoll, R. S., McKellar, J. L., et al. (2018). U-Pb geochronology and palynology from Lopingian (upper Permian) coal measure strata of the Galilee Basin, Queensland, Australia. *Aust. J. Earth Sci.* 65, 153–173. doi:10.1080/08120099.2018.1418431

Phillips, L. J., Esterle, J. S., and Edwards, S. A. (2017). Review of Lopingian (upper Permian) stratigraphy of the Galilee Basin, Queensland, Australia. *Aust. J. Earth Sci.* 64, 283–300. doi:10.1080/08120099.2017.1290684

Pinetown, K. L. (2014). Regional coal seam gas distribution and burial history of the Hunter Coalfield, Sydney Basin. *Aust. J. Earth Sci.* 61, 409–426. doi:10.1080/08120099.2014.893539

Potonié, R. and Lele, K. M. (1961). Studies in the Talchir Flora of India, 1. Sporae dispersae from the Talchir beds of South Rewa Gondwana Basin. *Palaeobotanist* 8, 22–37.

Price, P. L. (1997). "Permian to Jurassic palynostratigraphic nomenclature of the Bowen and Surat basins," in *The Surat and Bowen basins, Southeast Queensland*. Editor P. M. Green (Brisbane, Australia: Queensland Department of Mines and Energy), 137–178.

Rampino, M. R. and Eshet, Y. (2018). The fungal and acritarch events as time markers for the latest Permian mass extinction: an update. *Geosci. Front.* 9, 147–154. doi:10.1016/j.gsf.2017.06.005

Rattigan, J. and McKenzie, P. J. (1969). "History of sedimentation in the Sydney Basin: A. Hunter Valley," in *The Geology of New South Wales*. V. The Sydney Basin Editor G. H. Packham (Sydney: Geological Society of Australia), 426–434.

Retallack, G. J. (1977). Reconstructing Triassic vegetation of eastern Australasia: a new approach for the biostratigraphy of Gondwanaland. *Alcheringa* 1, 247–278. doi:10.1080/03115517708527763

Retallack, G. J. (1996). Early Triassic therapsid footprints from the Sydney Basin, Australia. *Alcheringa* 20, 301–314.

Retallack, G. J. (1999). Post-apocalyptic greenhouse paleoclimate revealed by earliest Triassic paleosols in the Sydney Basin, Australia. *Geol. Soc. Am. Bull.* 111, 52–70. doi:10.1130/0016-7606(1999)111<0052:PGPRBE>2.3.CO;2

Retallack, G. J. (1980). "Late Carboniferous to Middle Triassic megafossil floras from the Sydney Basin," in *Geology of the Sydney Basin*. Editors R. Helby and C. Herbert (Sydney: New South Wales Geological Survey Bulletin), Vol. 26, 384–430.

Retallack, G. J. (2002). *Lepidopteris callipteroides*, an earliest Triassic seed fern of the Sydney Basin, southeastern Australia. *Alcheringa* 26, 475–500. doi:10.1080/03115510208619538

Retallack, G. J. (2005). Earliest Triassic claystone breccias and soil-erosion crisis. *J. Sediment. Res.* 75, 679–695. doi:10.2110/jsr.2005.055

Retallack, G. J. (2018). Leaf preservation in *Eucalyptus* woodland as a model for sclerophyll fossil floras. *Alcheringa* 43, 71–84. doi:10.1080/03115518.2018.1457180

Retallack, G. J., Jahren, A. H., Sheldon, N. D., Chakrabarti, R., Metzger, C. A., and Smith, R. M. H. (2005). The Permian–Triassic boundary in Antarctica. *Antarct. Sci.* 17, 241–258. doi:10.1017/S0954102005002658

Retallack, G. J. and Krull, E. S. (2010). Landscape ecological shift at the Permian–Triassic boundary in Antarctica. *Aust. J. Earth Sci.* 46, 785–812. doi:10.1046/j.1440-0952.1999.00745.x

Retallack, G. J., Smith, R. M. H., and Ward, P. D. (2003). Vertebrate extinction across Permian–Triassic boundary in Karoo Basin, South Africa. *Geol. Soc. Am. Bull.* 115, 1133–1152. doi:10.1130/B25215.1

Retallack, G. J., Veevers, J. J., and Morante, R. (1996). Global coal gap between Permian–Triassic extinction and Middle Triassic recovery of peat-forming plants. *Geol. Soc. Am. Bull.* 108, 195–207. doi:10.1130/0016-7606(1996)108<0195:GCGBPT>2.3.CO;2

Rowe, H., Hughes, N., and Robinson, K. (2012). The quantification and application of handheld energy-dispersive x-ray fluorescence (ED-XRF) in mudrock chemostratigraphy and geochemistry. *Chem. Geol.* 324–325, 122–131. doi:10.1016/j.chemgeo.2011.12.023

Saxena, A., Singh, K. J., Cleal, C. J., Chandra, S., Goswami, S., and Shabbar, H. (2018). Development of the *Glossopteris* flora and its end Permian demise in the Tatapani–Ramkola Coalfield, Son–Mahanadi Basin, India. *Geol. J.* 54, 2472–2494. doi:10.1002/gj.3307

Scheibner, E. and Basden, H. (1998). *Geology of New South Wales—synthesis. Volume 2, geological evolution, memoir (Geology) 13*. (Sydney: Geological Survey of New South Wales).

Schneebeli-Hermann, E. and Bucher, H. (2015). Palynostratigraphy at the Permian-Triassic boundary of the Amb section, Salt Range, Pakistan. *Palynology* 39, 1–18. doi:10.1080/01916122.2014.921648

Seward, A. C. (1934). Some early Mesozoic plants from Tanganyika territory. *Geol. Mag.* 71, 387–392.

Sheldon, N. D. and Tabor, N. J. (2009). Quantitative paleoenvironmental and paleoclimatic reconstruction using paleosols. *Earth-Sci. Rev.* 95, 1–52. doi:10.1016/j.earscirev.2009.03.004

Shi, G. R., Waterhouse, J. B., and McLoughlin, S. (2010). The Lopingian of Australasia: a review of biostratigraphy, correlations, palaeogeography and palaeobiogeography. *Geol. J.* 45, 230–263. doi:10.1002/gj.1213

Sidor, C. A., Miller, M. F., and Isbell, J. L. (2008). Tetrapod burrows from the Triassic of Antarctica. *J. Vert. Paleont.* 28, 277–284. doi:10.1671/0272-4634(2008)28[277:TBFTTO]2.0.CO;2

Slansky, J. M. (1985). Geochemistry of high-temperature coal ashes and the sedimentary environment of the New South Wales coals, Australia. *Int. J. Coal Geol.* 5, 339–376. doi:10.1016/0166-5162(85)90002-3

Sliwa, R., Esterle, J., Phillips, L., and Wilson, S. (2017). Final Report Australian Coal Industry Research Program Project C22028. Rangal supermodel 2015: the Rangal-Baralaba-Bandanna Coal Measures in the Bowen and Galilee basins. Brisbane, 79.

Smith, R. M. H., Rubidge, B. S., Day, M. O., and Botha, J. (2020). Introduction to the tetrapod biozonation of the Karoo Supergroup. *S. Afr. J. Geol.* 132, 131–140. doi:10.25131/sajg.123.0009

Smith, R. M. H. and Ward, P. D. (2001). Pattern of vertebrate extinctions across an event bed at the Permian-Triassic boundary in the Karoo Basin of South Africa. *Geology* 29, 1147–1150. doi:10.1130/0091-7613(2001)029<1147:POVEAA>2.0.CO;2

Spina, A., Cirilli, S., Utting, J., and Jansonius, J. (2015). Palynology of the Permian and Triassic of the Tesero and Bulla sections (Western Dolomites, Italy) and consideration about the enigmatic species *Reduviasporonites chalastus*. *Rev. Palaeobot. Palynol.* 218, 3–14. doi:10.1016/j.revpalbo.2014.10.003

Srivastava, S. C., Anand-Prakash, and Kar, R. (1997). Palynology of Permian-Triassic sequence in Iria Nala, Tatapani-Ramkola Coalfield, India. *Palaeobotanist* 46, 75–80.

Standing Committee on Coalfield Geology of NSW (1975). Stratigraphy of the Newcastle Coal Measures. *Geol. Surv. NSW Rec.* 16, 33–36.

Steiner, M. B., Eshet, Y., Rampino, M. R., and Schwindt, D. M. (2003). Fungal abundance spike and the Permian–Triassic boundary in the Karoo Supergroup (South Africa). *Palaeogeog. Palaeoclimatol. Palaeoecol.* 194, 405–414. doi:10.1016/S0031-0182(03)00230-X

Stephenson, A. E. and Burch, G. J. (2004). *Preliminary evaluation of the petroleum potential of Australia's central eastern margin, Geoscience Australia, Records 2004/06*. Canberra: Geoscience Australia.

Stuntz, J. (1965). Petroleum exploration in the Sydney Basin. *APEA J.* 5, 59–62.

Tadros, N. Z. (1995). "Sydney-Gunnedah Basin overview," in *Geology of Australian Coal Basins*. Editors C. R. Ward, H. J. Harrington, C. W. Mallett, and J. W. Beeston (Sydney: Geological Society of Australia, Coal Geology Group, Special Publication), Vol. 1, 163–175.

Tewari, R., Awatar, R., Pandita, S. K., McLoughlin, S., Agnihotri, D., Pillai, S. S. K., et al. (2015). The Permian–Triassic palynological transition in the Guryul Ravine section, Kashmir, India: implications for Tethyan–Gondwanan correlations. *Earth-Sci. Rev.* 149, 53–66. doi:10.1016/j.earscirev.2014.08.018

Tillyard, R. J. (1918). A fossil insect wing from the roof of the coal seam in the Sydney Harbour Colliery. *Proc. Linn. Soc. NSW* 43, 260–264.

Townrow, J. A. (1956). The genus *Lepidopteris* and its Southern Hemisphere species. *Avhand. Norske Vidensk.-Akad. Oslo. I. Math.-Naturwiss.* 2, 1–28.

Townrow, J. A. (1957). On *Dicroidium*, probably a pteridospermous leaf, and other leaves now removed from this genus. *Trans. Geol. Soc. S. Afr.* 60, 21–56.

Townrow, J. A. (1960). The Peltaspermaceae, a pteridosperm family of Permian and Triassic age. *Palaeontology* 3, 333–361.

Townrow, J. A. (1966). On *Lepidopteris madagascariensis* carpentier (Peltaspermaceae). *J. Proc. Roy. Soc. NSW* 98, 203–214.

Townrow, J. A. (1967a). On *Rissikia* and *Mataia*, podocarpaceous conifers from the lower Mesozoic of southern lands. *Pap. Proc. Roy. Soc. Tas.* 101, 103–138.

Townrow, J. A. (1967b). On *Voltziopsis*, a southern conifer of Lower Triassic age. *Pap. Proc. Roy. Soc. Tas.* 101, 173–188.

Uren, R. E. (1974). Report 2 (unpublished), GS19741431. The geology of low cost extractive resources of the Gosford-Lake Macquarie area. Geological Survey of New South Wales.

Vajda, V. and Bercovici, A. (2014). The global vegetation pattern across the Cretaceous–Paleogene mass extinction interval: a template for other extinction events. *Global Planet. Change* 122, 29–49. doi:10.1016/j.gloplacha.2014.07.014

Vajda, V. and McLoughlin, S. (2007). Extinction and recovery patterns of the vegetation across the Cretaceous–Palaeogene boundary—a tool for unravelling the causes of the end-Permian mass-extinction. *Rev. Palaeobot. Palynol.* 144, 99–112. doi:10.1016/j.revpalbo.2005.09.007

Vajda, V., McLoughlin, S., Mays, C., Frank, T., Fielding, C. R., Tevyaw, A., et al. (2020). End-Permian (252 Mya) deforestation, wildfires and flooding—an ancient biotic crisis with lessons for the present. *Earth Planet. Sci. Lett.* 529, 115875. doi:10.1016/j.epsl.2019.115875

Veevers, J. J. (2006). Updated Gondwana (Permian–Cretaceous) earth history of Australia. *Gondwana Res.* 9, 231–260. doi:10.1016/j.gr.2005.11.005

Ward, C. R. (1972). Sedimentation in the Narrabeen Group, southern Sydney Basin, New South Wales. *J. Geol. Soc. Aust.* 19, 393–409. doi:10.1080/00167617208728809

Ward, P. D., Botha, J., Buick, R., Kock, M. O. D., Erwin, D. H., Garrison, G. H., et al. (2005). Abrupt and gradual extinction among Late Permian land vertebrates in the Karoo Basin, South Africa. *Science* 307, 709–714. doi:10.1126/science.1107068

Warren, A. (1997). A tetrapod fauna from the Permian of the Sydney Basin. *Rec. Aust. Mus.* 49, 25–33. doi:10.3853/J.0067-1975.49.1997.297

Wheeler, A. (2020). Spatiotemporal variation in the Permian-Triassic pre- and post-extinction palynology of the Bowen and Galilee basins (Australia). The University of Queensland, Brisbane. PhD thesis.(unpublished)

Wheeler, A., Van de Wetering, N., Esterle, J. S., and Götz, A. E. (2020). Palaeoenvironmental changes recorded in the palynology and palynofacies of a late Permian marker mudstone (Galilee Basin, Australia). *Palaeoworld* 29, 439–452. doi:10.1016/j.palwor.2018.10.005

White, M. E. (1981). *Cylomeia undulata* (Burges) gen. et comb. nov., a lycopod of the Early Triassic strata of New South Wales. *Rec. Aust. Mus.* 33, 723–734.

Williams, M. L., Jones, B. G., and Carr, P. F. (2017). The interplay between massive volcanism and the local environment: geochemistry of the Late Permian mass extinction across the Sydney Basin, Australia. *Gondwana Res.* 51, 149–169. doi:10.1016/J.GR.2017.07.015

Wu, Y., Tong, J., Algeo, T. J., Chu, D., Cui, Y., Song, H., et al. (in press 2019). Organic carbon isotopes in terrestrial Permian-Triassic boundary sections of North China: implications for global carbon cycle perturbations. *Geol. Soc. Am. Bull.*

Xu, J. F. and Ward, C. R. (1993). "Triassic depositional episode," in *The Gunnedah Basin, New South Wales*. Editor N.Z. Tadros (Sydney: Geological Survey of New South Wales, Memoir Geology), Vol. 12, 297–326.

Yago, J. V. R., Fielding, C. R., and Lodwick, W. (2015). "Depositional environments and sediment dispersal patterns of the Jurassic Walloon Subgroup in eastern Australia," in *Eastern Australasian Basins Symposium, A powerhouse emerges: energy for the next fifty years*, 141–150.

Yoo, E. K., Norman, A., and McDonald, I. (1995). "Sydney Basin—Western Coalfield," in *Geology of Australian coal basins*. Editors C. R. Ward, H. J. Harrington, C. W. Mallett, and J. W. Beeston (Sydney: Geological Society of Australia, Coal Geology Group, Special Publication), Vol. 1, 231–245.

**Conflict of Interest:** Author MB was employed by the geological consultancy company Bocking Associates CBM Pty Ltd.

The remaining authors declare that the research was conducted in the absence of any commercial or financial relationships that could be construed as a potential conflict of interest.

The handling editor declared a past co-authorship with several of the authors (VV, SM).